AD-A082 079 MAINE UNIV ORONO DEPT OF ELECTRICAL ENGINEERING F/G 9/3
MICROWAVE SURFACE ACOUSTIC WAVE MATERIALS.(U)
FEB 80 J F VETELINO AFOSR-75-2816
UNCLASSIFIED AFOSR-TR-80-0135 NL

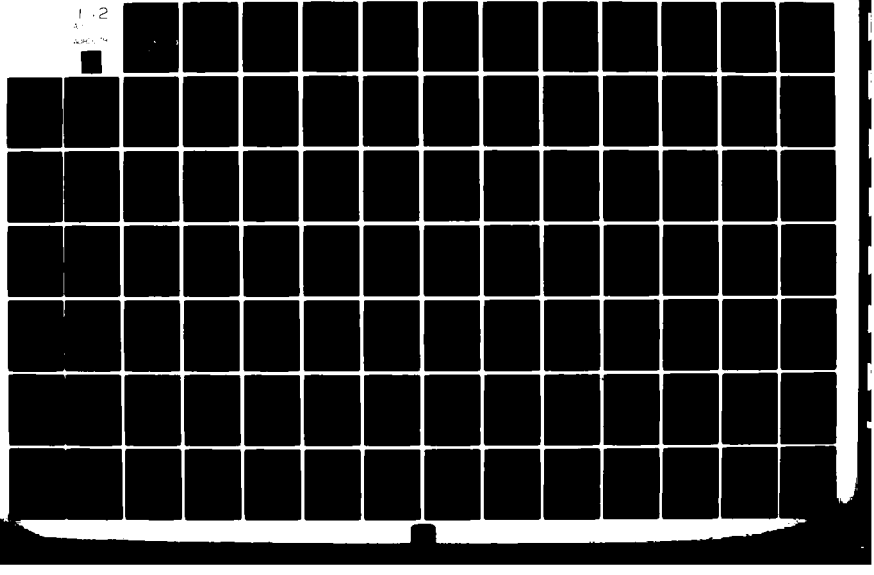

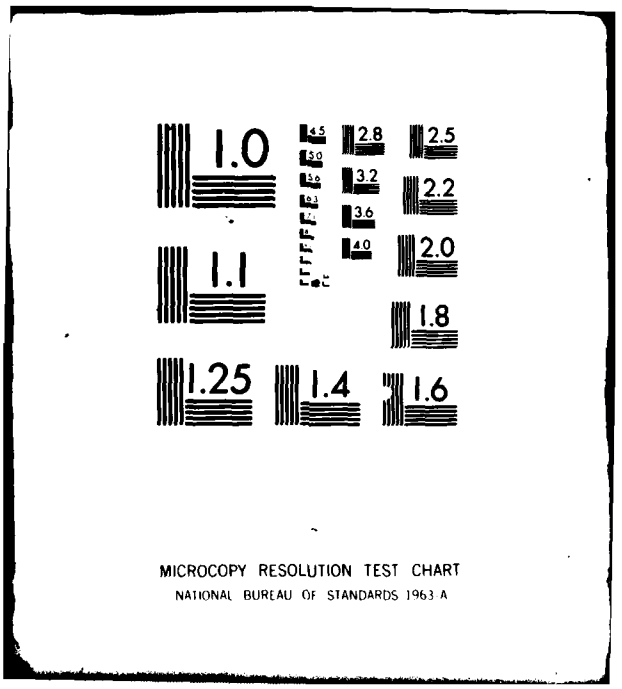
1.0
1.1
1.25
1.4
1.6
1.8
2.0
2.2
2.5
2.8
3.2
3.6
4.0
4.5
5.0
5.6
6.3
7.1
MICROCOPY RESOLUTION TEST CHART
NATIONAL BUREAU OF STANDARDS 1963 A

AFOSR-TR- 80-0135

(12)

LEVEL II

AD A082079

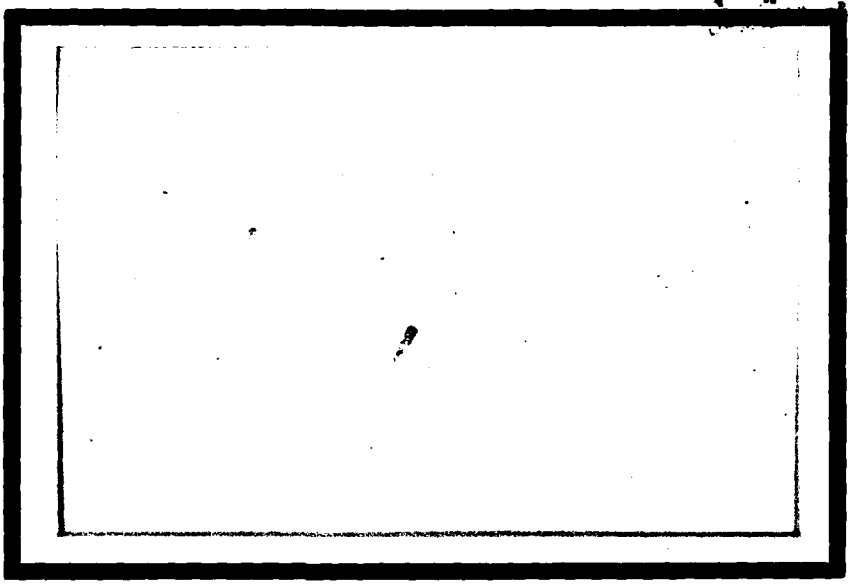

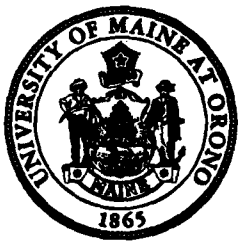

DTIC
ELECTE
MAR 17 1980
S D
A

DEPARTMENT OF ELECTRICAL ENGINEERING

UNIVERSITY OF MAINE AT ORONO

DDC FILE COPY

Approved for public release;
distribution unlimited.

80 3 14 051

MICROWAVE SURFACE ACOUSTIC WAVE MATERIALS

J.F. Vetelino
Principal Investigator

Final Scientific Report
February 1980

Contract Number AFOSR 75-2816

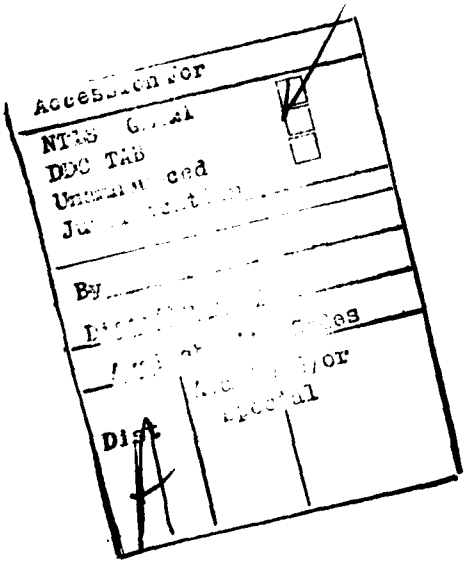

REPORT DOCUMENTATION PAGE

READ INSTRUCTIONS BEFORE COMPLETING FORM

1. REPORT NUMBER: AFOSR-TR-80-0135	2. GOVT ACCESSION NO.
3. RECIPIENT'S CATALOG NUMBER	
4. TITLE (and Subtitle): Microwave Surface Acoustic Wave Materials.	5. TYPE OF REPORT & PERIOD COVERED: Final Report Feb. 15, 1975 - June 1, 1979
	6. PERFORMING ORG. REPORT NUMBER
7. AUTHOR(s): John F. Vetelino	8. CONTRACT OR GRANT NUMBER(s): AFOSR-75-2816
9. PERFORMING ORGANIZATION NAME AND ADDRESS: Department of Electrical Engineering, University of Maine, Orono, Maine 04469	10. PROGRAM ELEMENT, PROJECT, TASK AREA & WORK UNIT NUMBERS: 2306/B1, 61102F
11. CONTROLLING OFFICE NAME AND ADDRESS: Department of the Air Force, Air Force Office of Scientific Research (AFOSR), Bolling Air Force Base, Washington D.C. 20332	12. REPORT DATE: FEB 1980; NUMBER OF PAGES: 101
14. MONITORING AGENCY NAME & ADDRESS (if different from Controlling Office): Final rept. 15 Feb 75 - 1 Jun 79,	15. SECURITY CLASS. (of this report): Unclassified
	15a. DECLASSIFICATION/DOWNGRADING SCHEDULE

16. DISTRIBUTION STATEMENT (of this Report)

Approved for public release; distribution unlimited.

16 2306

17 1B

17. DISTRIBUTION STATEMENT (of the abstract entered in Block 20, if different from Report)

18. SUPPLEMENTARY NOTES

19. KEY WORDS (Continue on reverse side if necessary and identify by block number)

Ultrasonics	Surface skimming waves	Bleustein Gulyaev Modes
Microwave acoustics	Plate modes	Diffraction
Surface acoustic waves	Love modes	Temperature compensated materials
Surface acoustic wave properties	Rayleigh modes	
Pseudo surface acoustic waves	Layered structures	

(over)

20. ABSTRACT (Continue on reverse side if necessary and identify by block number)

Please refer to attached page for abstract

B

410635

DD FORM 1473 14/3 EDITION OF 1 NOV 65 IS OBSOLETE

UNCLASSIFIED

SECURITY CLASSIFICATION OF THIS PAGE (When Data Entered)

UNCLASSIFIED

(19 cont'd.)

Piezoelectric crystals	Lithium Gallium oxide	Fuzed quartz on $LiNbO_3$
Berlinite	Lithium iodate	Gold on quartz
Lead Potassium niobate	Lithium niobate	Aluminum on quartz
Bismuth Silicon oxide	α-Iodic acid	Metallic layers on quartz
Bismuth Germanium oxide	Fresnoite	Metallic layers on $LiNbO_3$
Sulfosalt materials	Selenium	

Unclassified

(20) Unclassified

The acoustic wave properties of several piezoelectric crystals and a layered structure have been theoretically and experimentally investigated for possible application in microwave acoustic devices. A search was made for crystals and layered structures having one or more of the following properties: (i) temperature compensation, (ii) high piezoelectric coupling, (iii) low power flow angle, (iv) low loss and (v) low or high acoustic wave velocities. The acoustic waves studied were the bulk acoustic waves (BAW), the surface acoustic waves (SAW), the pseudo SAW (PSAW), the plate modes and the surface skimming bulk waves (SSBW). The wave properties studied were the velocity, piezoelectric coupling, the temperature coefficient of delay, diffraction and attenuation.

In addition to the standard SAW materials such as α-quartz, $LiNbO_3$, $Bi_{12}GeO_{20}$ and $LiTaO_3$ the other single crystals studied were $LiGaO_2$, $LiIO_3$, α-HIO_3, α-$AlPO_4$, Tl_3VS_4, Tl_3TaSe_4, Se, $Pb_2KNb_5O_{15}$, $Ba_2Si_2TiO_8$ and $Bi_{12}SiO_{20}$. $LiGaO_2$ was found to be similar to $LiTaO_3$. $LiIO_3$ combined very high coupling with low SAW velocities (~ 2000 m/sec). Tl_3VS_4 and Tl_3TaSe_4 were found to have good coupling, temperature compensation and low SAW velocities (~ 1000 m/sec). α-$AlPO_4$ was found to have many temperature compensated cuts with zero power flow and coupling higher than quartz. $Ba_2Si_2TiO_8$ with its low dielectric constants and reasonable coupling, was found to be particularly attractive for convolver applications. $Bi_{12}SiO_{20}$ was found to be similar to $Bi_{12}GeO_{20}$.

The layered geometries examined studied included fused silica on $LiNbO_3$ and gold, aluminum and copper layers on quartz. The overlay structures were found to be more temperature stable than the single crystals.

A theory describing the spectrum of acoustic waves emanating from an interdigital transducer was developed. Several promising cuts for SSBW in quartz were identified and studied both theoretically and experimentally. Finally, various prototype SSBW devices were fabricated and tested.

UNCLASSIFIED

SECURITY CLASSIFICATION OF THIS PAGE (When Data Entered)

TABLE OF CONTENTS

I. RESEARCH OBJECTIVES

The increased use of surface acoustic wave (SAW) devices in microwave systems has created a need for new piezoelectric crystals, further study on composite materials such as thin film overlay configurations and a study of acoustic waves such as pseudo SAWs and surface skimming bulk waves (SSBW). The crystals and composite materials are needed in SAW devices such as delay lines, filters, encoders, decoders and related microwave signal processing devices. In addition, the study of composite materials is especially relevant to the development of the state of the art in monolithic integrated microwave circuits containing both SAW and semiconductor devices. There are several important features which one can look for in either the crystal or composite material which might prove to be important in a corresponding device and/or microwave integrated circuit application. Some of these properties are (i) one or more temperature compensated orientations for which the temperature coefficient of the transit time of the surface wave is zero, (ii) high piezoelectric coupling, (iii) low loss in the surface acoustic wave, (iv) a low power flow angle associated with the surface wave and (v) very low (<1000 m/sec) or high (>6000 m/sec) surface wave velocities, (vi) a composite material having a frequency dispersion useful in a dispersive SAW device such as a dispersive delay line or filter and/or capable of integrating both SAW and semiconductor devices on a common substrate. Another possible approach to satisfy the need for better microwave acoustic devices is to use waves such as the pseudo SAW or SSBW instead of the SAW to transmit the information in the piezoelectric crystal. These types of waves may be more suitable in terms of the aforementioned properties.

The major research objectives of this work are as follows: (i) to perform theoretical studies on a large number of piezoelectric single crystals in order to see if any of these crystals exhibit one or more of the first five features listed above, (ii) to theoretically and experimentally study various thin film overlay configurations in order to see if any of these configurations satisfy one or more of the above properties, (iii) to perform an experimental investigation of the SAW properties of α - $AlPO_4$ (berlinite) in order to evaluate its potential in SAW applications requiring temperature stability and (iv) to initiate a theoretical and experimental study on SSBW to see if these waves are more useful than SAWs in microwave acoustic applications. The surface wave velocity, the coefficient of time delay, the piezoelectric coupling and the power flow angle are all to be theoretically and/or experimentally determined for objectives (i) and (ii). Berlinite is particularly interesting since theoretical calculations have shown it to be temperature compensated and possess about four times the coupling of α - quartz. Various berlinite samples are to be characterized with respect to elemental composition, structural purity and crystallographic orientation. Electrode patterns will be deposited on berlinite and experimental investigations of SAW properties such as velocity, coupling, temperature coefficient of delay, diffraction, power flow angle and attenuation will be performed. Definite conclusions are to be given as to the merit of using berlinite for SAW applications requiring temperature stability. Finally, work will be initiated on SSBW to ascertain their value in microwave acoustic applications.

The funding for the work on single crystals (objective (i)) began on February 15, 1975, while funding for the theoretical work on thin film overlays (objective (ii)) was requested for in a renewal proposal and began on July 1, 1976. Funding appropriate for the work on berlinite was requested in an

amendment proposal to the original grant. The berlinite work started on June 1, 1977. The experimental work on thin film overlays and the initiation of the SSBW work began in July 1, 1978. The SSBW work has been under the sponsorship of the National Science Foundation (NSF) since June, 1979.

II. SIGNIFICANT ACCOMPLISHMENTS

A. Introduction

A significant amount of theoretical work pursuant to the objectives has been performed to date. The experimental work includes the fabrication of a berlinite SAW device, the development of a laser system to measure SAW diffraction profiles, the fabrication and property measurements of several overlay configurations and the fabrication and property measurements of some SSBW devices.

Currently, the SAW group at the University of Maine has the theoretical capability to completely characterize the SAW and pseudo SAW properties of a candidate piezoelectric material given the input material constants such as the elastic, piezoelectric and dielectric constants. The SAW group also has the theoretical ability to characterize the modes appropriate for a layered geometry. Work was also begun on the analysis and use of SSBWs for microwave acoustic device applications.

Several computer programs were developed during the AFOSR contract period. Among these are:

(i) A program to calculate the SAW velocity, electromagnetic to acoustic coupling ($\Delta v/v$), power flow angle and temperature coefficient of delay (TCD) as a function of crystallographic orientation given the material's properties.

(ii) A program to calculate the SAW properties described in (i) for a pseudo SAW. This program also calculates the attenuation of the pseudo SAW.

(iii) A program to calculate the SAW properties described in (i) for the various modes which can exist in a layered media.

(iv) A program to calculate the characteristics of plate modes.

(v) A program to calculate the characteristics of bulk electromagnetic and acoustic waves.

(vi) A program to calculate SAW diffraction profiles and diffraction losses.

Preliminary work was begun under the AFOSR contract on the theory of SSBWs and is now being continued under NSF sponsorship.

In the following sections a summary of the work performed persuant to the program objectives is described.

B. Single Crystals

The SAW, and in some cases the pseudo SAW properties; were determined for $LiGaO_3$, $LiIO_3$, α-HIO_3, α-$AlPO_4$ (berlinite), $Bi_{12}SiO_{20}$ (BSO), Se, $Pb_2KNb_5O_{15}$ (PKN), Tl_3TaSe_4, Tl_3VS_4 and $Ba_2Si_2TiO_8$. Some of the important results and appropriate discussion of these materials is presented next.

Lithium Gallium Oxide

$LiGaO_2$ belongs to the orthorhombic crystal system and to the C_{2v} point group. It was one of the first materials investigated because one of its elastic constants was known to have a positive temperature derivative. Using the data of Nanamatsu *et al*[1] the SAW parameters were calculated. The variations of these parameters are presented in Figures 1 and 2. The crystallographic cuts have been connected so that it is possible to present a continuous variation for the quantities of interest.

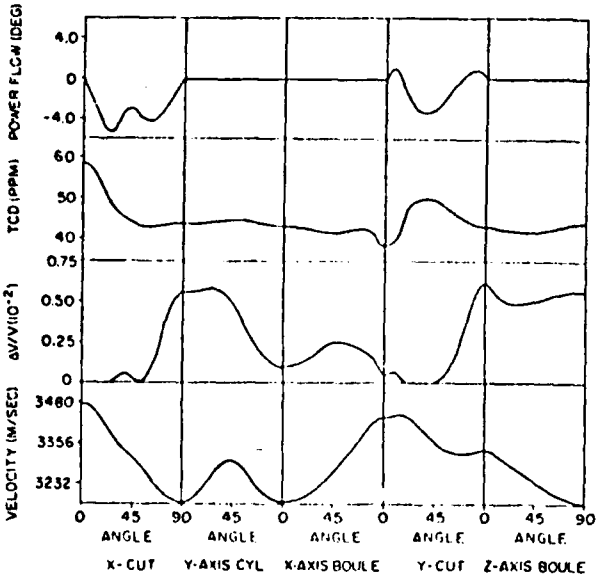

FIG. 1. The variation of the SAW velocity, TCD, $\Delta v/v$, and the power flow angle for x- and y-cut, x- and z-axis boule and y-axis cylinder $LiGaO_2$.

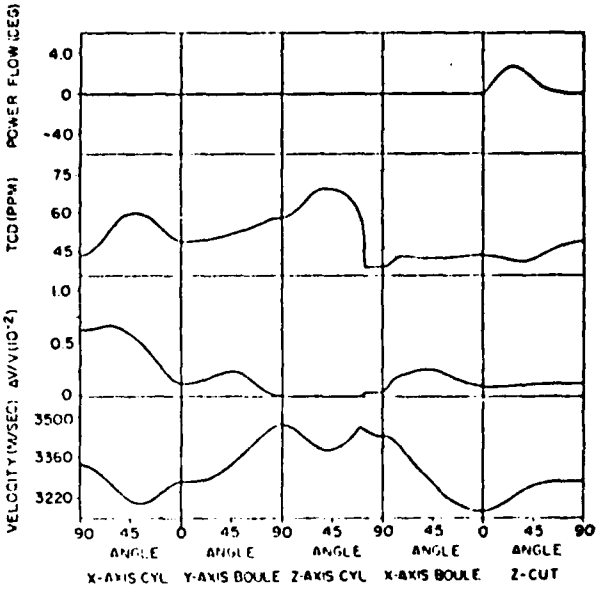

FIG. 2. The variation of the SAW velocity, TCD, $\Delta v/v$, and the power flow angle for z-cut, x- and y-axis boule and x- and z-axis cylinder $LiGaO_2$.

The SAW velocity varies from 3173 m/sec at x-cut ($\theta=90^o$) to 3474.5 m/sec at x-cut ($\theta=0^o$), y-axis boule ($\theta=90^o$) and z-axis cylinder ($\theta=0^o$). The maximum value for $\Delta v/v$ was 0.66×10^{-2} and occurred for the x-axis cylinder ($\theta=55^o$). The lowest TCD value was 38.2 ppm along the z-axis cylinder cut ($\theta=15^o$). $LiGaO_2$ has a zero power flow angle along the x-, y- and z-axis boule and cylinder cuts. Qualitatively, $LiGaO_2$ seems to compare most closely to $LiTaO_3$. However, it seems to be inferior to $LiTaO_3$ in that $LiGaO_2$ has a higher minimum TCD and a slightly lower maximum $\Delta v/v$.

The nonexistence of a temperature-compensated cut was a little surprising at first since $LiGaO_2$ possesses an elastic constant with a positive temperature derivative.

A criterion that has been used[2] as a hint to a possible temperature-compensated cut has been the existence of a positive temperature derivative of an elastic constant. If the material is not piezoelectric, this criteria seems to work since the surface wave velocity is primarily a function of the elastic constants. This has also been found to work in quartz and TeO_2[3], which possess low piezoelectric coupling. However, this concept does not work in $LiGaO_2$. In quartz and TeO_2 the mechanical and electromagnetic wave equations are weakly coupled due to the low piezoelectric coupling. Therefore, the neglect of piezoelectric effects is a good approximation. In $LiGaO_2$ the piezoelectric coupling is fairly high in comparison to that of quartz and TeO_2, therefore, the mechanical and electromagnetic wave equations are more strongly coupled. On the basis of this, one might conclude that a more correct criteria should include the temperature dependence of the dielectric and piezoelectric constants in addition to the temperature dependence of the elastic constants.

Lithium Iodate

$LiIO_3$ belongs to the hexagonal crystal system with point symmetry, C_6 and space group $P6_3$. Haussühl[4] measured its dielectric, piezoelectric and elastic constants along with their temperature derivatives. The SAW velocity, piezoelectric coupling, TCD and power flow angles were calculated[5,6] for the X, Y and Z cuts, along with the cylinder and boule cuts. The results are presented in Figure 3. The cuts have been connected so that there is a continuous variation for the quantitites of interest. The values for the Z type cuts, i.e., Z-cut, Z-axis boule, and Z-axis cylinder, are not shown but may be deduced from Figure 3. Because of the hexagonal symmetry of the $LiIO_3$ lattice,

there is no variation in SAW properties over any of these cuts. The values for the SAW properties of Z-cut are those of X- and Y-axis cylinder at 0^{o}, for Z-axis boule they are those of X- and Y-cut at 90^{o}, while for Z-axis cylinder they are those of X- and Y-axis boule at 90^{o}.

As is obvious from Figure 3, the most attractive cut for this material is Z-cut where the SAW properties remain constant over the entire cut. The SAW velocity is nearly 2240 m/sec, the coupling is 0.043 and the power flow angle is zero. The piezoelectric coupling for Z-cut is the highest coupling for a SAW reported so far for any material. However, the TCD at this cut is very high (264 ppm/^{o}C). The TCD values for $LiIO_3$ lie between 250 and 400 ppm/^{o}C depending upon the cut. A recent experimental investigation on $LiIO_3$

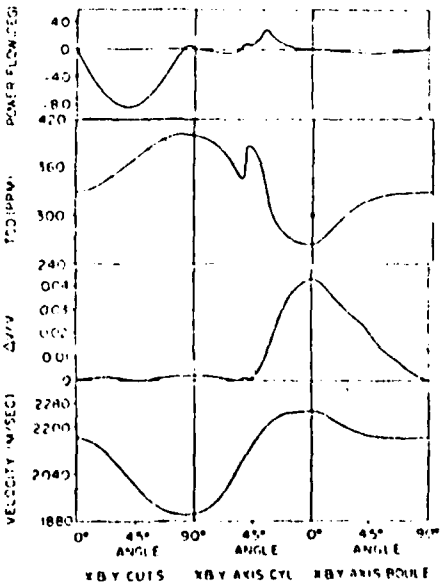

FIG. 3. SAW Properties of $LiIO_3$ for Various Crystallographic Directions. The Circle Denotes an Experimental Point (from ref. 6)

by Soluch et al.[6] has verified the above result on Z-cut. It should be mentioned here that the X- and Y-cut 90° solution is a Bleustein Gulyaev solution with mechanical motion perpendicular to the sagittal plane.

Due to the hygroscopic nature of this material, the commonly used photolithographic techniques for the transducer fabrication might give rise to some problems. For this reason, Soluch et al.[6] engraved the transducer on the crystal.

α-Iodic Acid

α-Iodic acid is an orthorhombic crystal with space group D_2^4. Several people, including Mason[7], Haussühl[8], Volkova et al.[9] have measured its piezoelectric constants, dielectric constants and elastic constants. These measurements differ considerably. The data presented by Haussühl was used for this work.

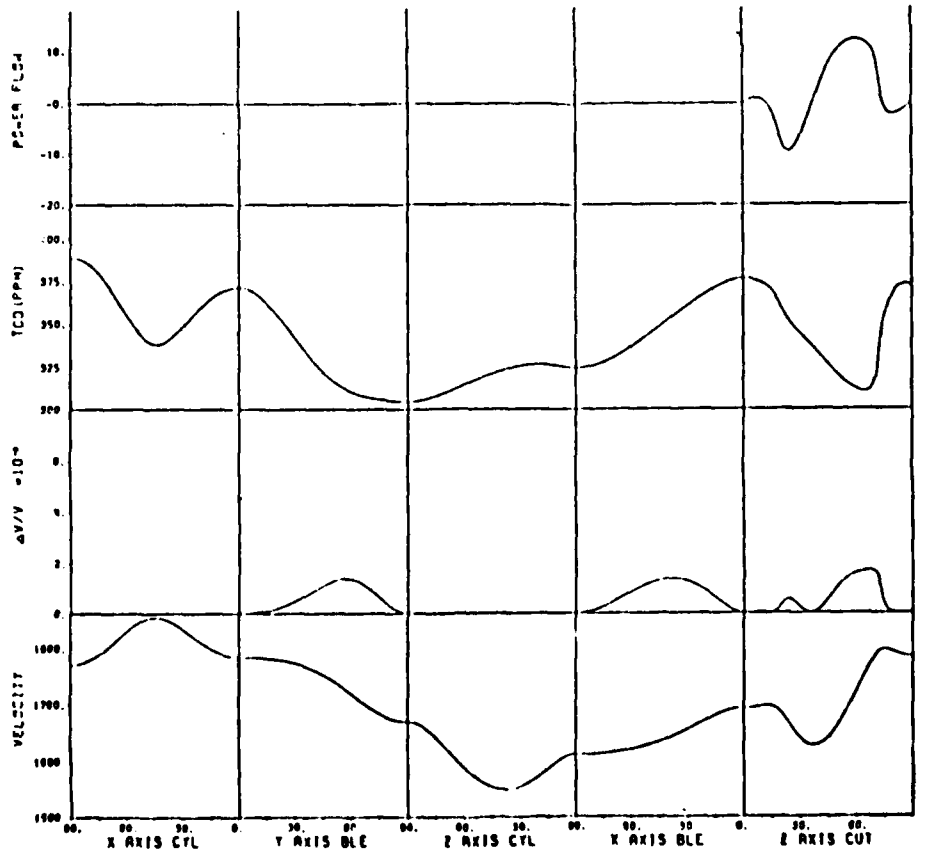

FIG. 4. SAW Properties of α-HIO_3 for Various Crystallographic Directions

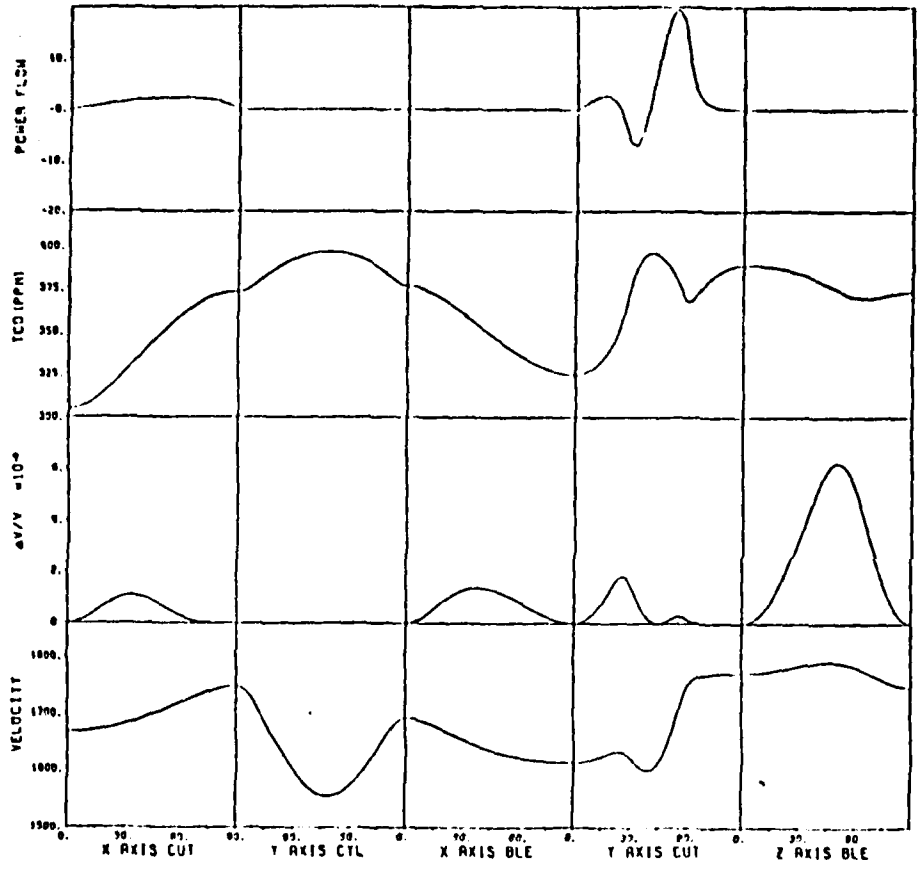

FIG. 5. SAW Properties of α-HIO_3 for Various Crystallographic Orientations

The complete results for α-HIO_3 are presented in Figures 4 and 5. The X, Y and Z-axis cylinder cut belongs to the 4 row 2 zero special case[10]. This solution has mechanical motion confined to the sagittal plane and has no coupling. The best crystallographic cut for this material is 45°, Z-axis boule. It has a velocity less than 1800 m/sec., coupling higher than 0.8×10^{-2} and zero power flow angle. The TCD value is approximately 380 ppm/°C which is quite high.

This material is highly hygroscopic in nature. The material, therefore, is not attractive for SAW applications as compared to those presently used.

Berlinite

The crystal structure of berlinite[11] is isomorphic to quartz. Half of the silicon positions are occupied by trivalent Al ions and half by pentavalent P ions. This results in an effective doubling of the unit cell along the c-axis. $AlPO_4$ can exist[12, 13] in a quartz-like or berlinite structure, a cristobalite structure and a tridymite structure. For many materials, these structural forms can exist[14] in a high temperature (β) or low temperature (α) phase. The most symmetrical bond linkages[15] are associated with the β-phase whereas the corresponding α-phase is a distortion or derivative structure. Recently, it has been shown[16] that a crystal undergoing this sort of displacive phase transition might have elastic constants which increase with temperature thereby rendering the crystal a promising candidate for temperature compensation.

The experimental data for the elastic, piezoelectric and dielectric constants and their temperature derivatives have been obtained from the work of Chang et al.[17]

The complete results of the SAW and pseudo SAW properties are presented in Figures 6 and 7. The SAW associated with the following list, namely, X-axis cylinder, Z-cut, 30^o and 90^o and Y-axis boule, 0^o, belongs to the special four row two zero case. The entire X-axis cylinder cut and the allowed SAW solutions on the pseudo SAW branch for Z-cut, 30^o and 90^o and Y-axis boule, 0^o, indicated by crosses in the figures, are a zero coupling type SAW. The solutions on the SAW branch for Z-cut, 30^o and 90^o, and Y-axis boule, 0^o, indicated by triangles in the figures are Bleustein-Gulyaev modes with one mode having a bulk propagation term.

First order pseudo SAW solutions were found to exist over certain regions in the nine crystallographic cuts. The points X-axis boule, 12^o, and Y-axis cylinder, 47.2^o, indicated by circles in the figure, are perfect SAW

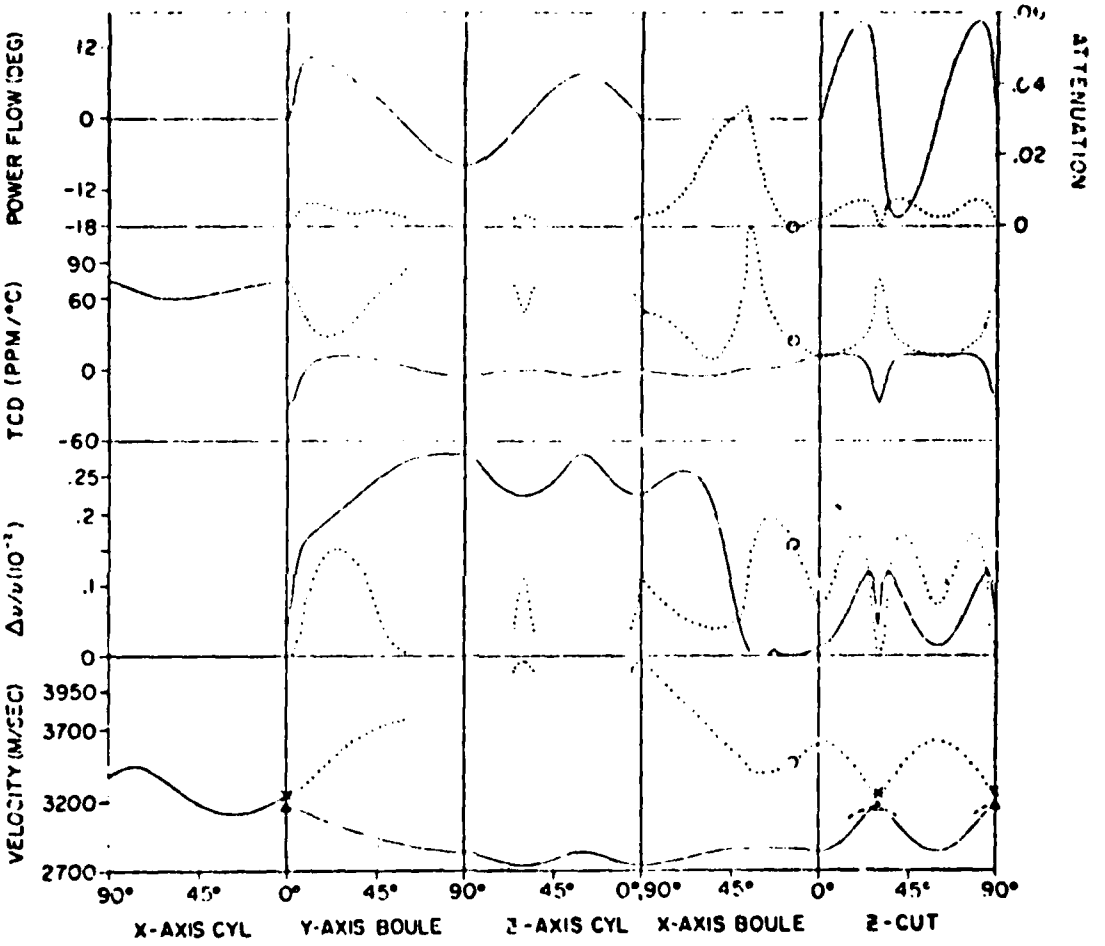

FIG. 6 SAW and Pseudo SAW Properties of Berlinite. Solid line: Properties Associated with SAW. Dotted Line: Properties Associated with Pseudo SAW. Dashed Line: Bulk Wave. Δ: Tilted Bulk Wave Satisfying Boundary Conditions. X: SAW Wave with Zero Coupling. O: Isolated SAW on Pseudo SAW Branch.

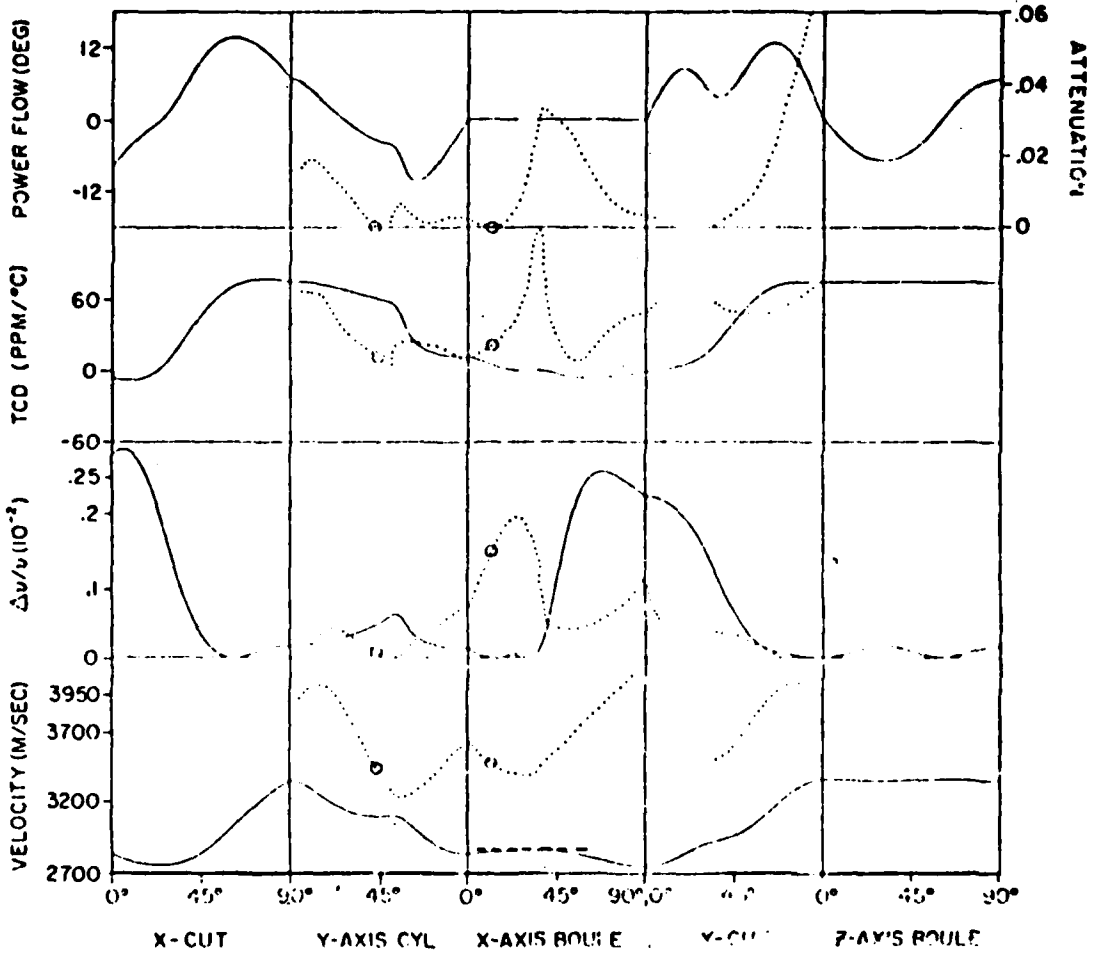

FIG. 7 SAW and Pseudo SAW Properties of Berlinite. Solid Line: Properties Associated with SAW. Dotted Line: Properties Associated with Pseudo SAW. Dashed Line: Bulk Wave. Δ: Tilted Bulk Wave Satisfying Boundary Conditions. X: SAW Wave with Zero Coupling. O: Isolated SAW on Pseudo SAW Branch.

solutions on the pseudo SAW branch. The attenuation of the pseudo SAW branch becomes zero at these points, hence rendering two perfect SAW solutions. The complete theory associated with first order and higher order pseudo SAWs may be found in a recent publication[10] by the University of Maine SAW group.

Berlinite was found to have several temperature compensated cuts. The coupling associated with these cuts was in some cases 4 times the coupling characteristic of α-quartz. The best point is X-axis boule, 92.75° which has a zero power flow angle, zero TCD, a coupling of 0.22×10^{-2} and a SAW velocity equal to 2733 m/sec.

Berlinite has definite possibilities for SAW device applications such as encoders, decoders[18] and related signal processing devices where temperature stability is important. Berlinite has been shown to have many temperature compensated cuts whose corresponding coupling is much higher than the coupling of commonly used α-quartz. It should also be pointed out that berlinite might be only one of many potentially temperature compensated materials with a silica derivative type structure.

Selenium

Trigonal selenium (sometimes classed as hexagonal) belongs to either the space group D_3^4 or D_3^6. The elastic, piezoelectric and dielectric constant measurements on this material have been done primarily by Shiosaki et al.[19], Araki et al[20], Vedam et al.[21] and Mort[22]. The measurements differ considerably, especially in the piezoelectric constants. The data that was used was thus of considerable uncertainty.

Some preliminary calculations on this material revealed a very low SAW velocity (800 m/sec to 1200 m/sec) and very high piezoelectric coupling (5.5×10^{-2}). SAW properties were calculated for several cuts but have not been yet completed. Accurate experimental measurements of the elastic and piezoelectric constants are required.

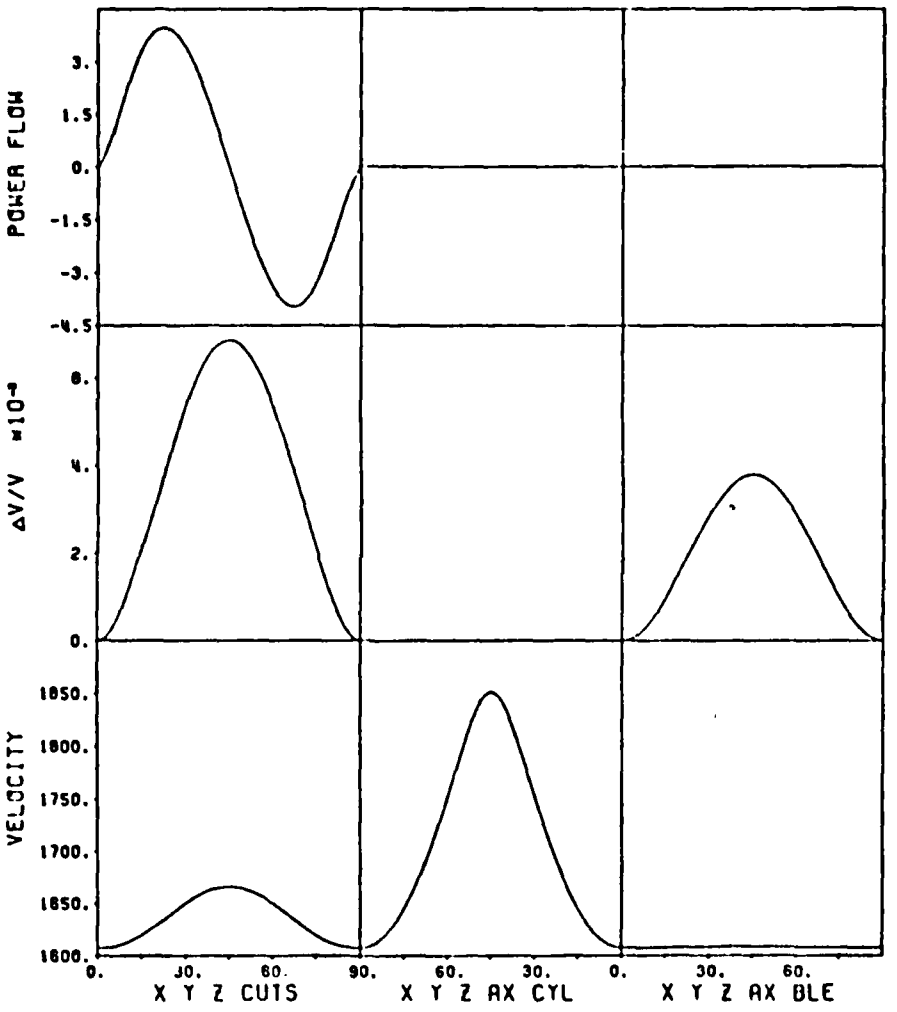

FIG. 8. SAW Properties of *BGO* for Various Crystallographic Orientations

The fact that this material is poisonous might hinder its use in applications.

Lead Potassium Niobate

Lead Potassium Niobate (PKN) is a ferroelectric crystal belonging to the space group Cm 2m (C_{2v}^{14}) at room temperature. Yamada[23] measured its elastic, dielectric and piezoelectric constants.

The SAW properties for several cuts were examined for this material. The piezoelectric coupling for some orientations were found to be as high as 7×10^{-2}. However, the calculations were not completed for the material.

In addition to its high coupling, this crystal has another interesting property. Bulk wave measurements[23] indicate a likelihood of the existence of temperature compensated cuts. But it is difficult to obtain large crystals of this material[24] applicable for SAW applications. Further experimental and theoretical work is required on this material.

Bismuth Germanium Oxide (BGO) and Bismuth Silicon Oxide (BSO)

Both BGO and BSO are cubic materials belonging to the point group 23. Work on the SAW properties of BGO have been done earlier by Pratt et al.[25], Kraut[26] and Slobodnik et al.[27] The material was found[28] to have a minimal diffraction cut. This material is also characterized by relatively low SAW velocities making it an excellent candidate for long delay lines. Since BSO is quite similar to BGO, a study of this material was undertaken. No TCD calculations were done due to the lack of sufficient temperature derivative data.

The data for the elastic, piezoelectric and dielectric constants for BSO were obtained from the work of Schweppe and Quadfleig[29]. Figures 8 and 9 present the variation of the SAW velocity, coupling and power flow angle for BGO and BSO respectively. The results of the two materials are strikingly similar. The cylinder cuts are 4 row and 2 zero cases with the solution having displacements only in the sagittal plane. The SAW velocities on the boule cuts are not constant, although it appears so in the figure due to the large scale. They

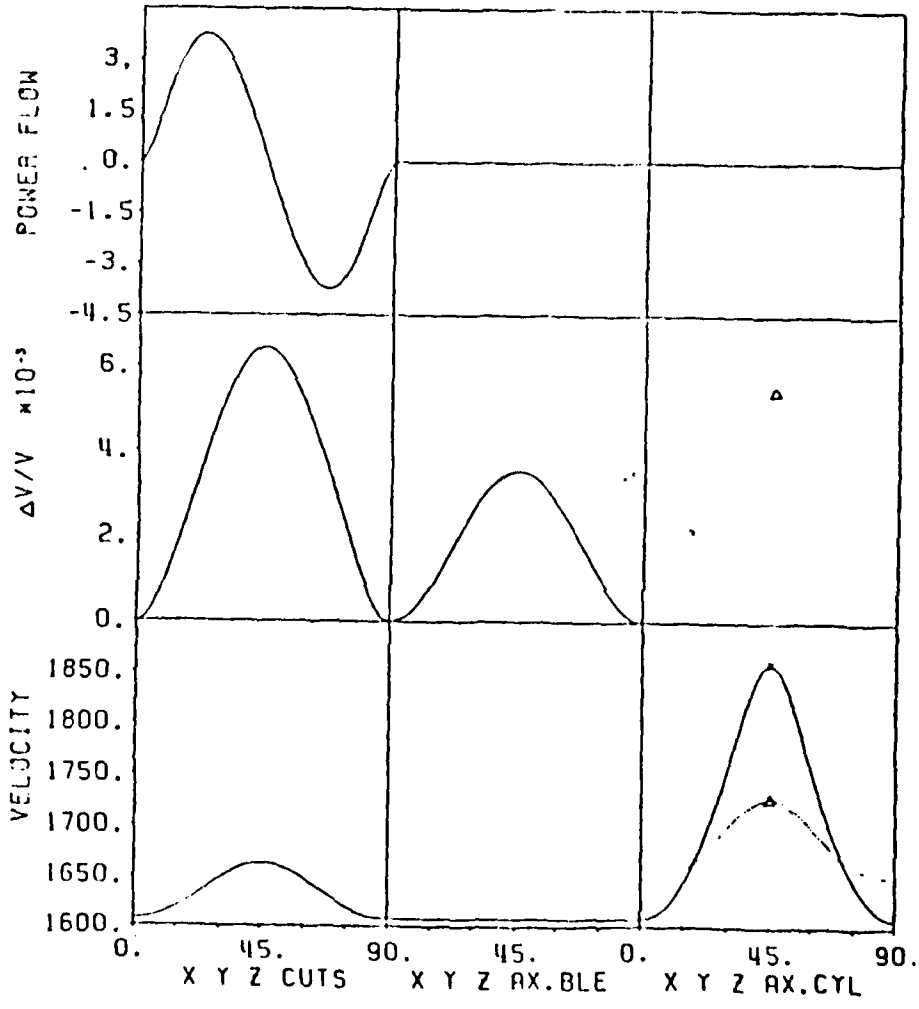

FIG. 9. The variation of the SAW velocity, $\Delta v/v$ and power flow angle for the X, Y and Z cut, X, Y and Z axis boule and X, Y and Z axis cylinder BSO. Solid line: properties associated with the SAW. Dotted line: velocity of the lowest shear mode. X: SAW mode with zero coupling. Δ: Bleustein-Gulyaev mode with propagation vector tilted into the bulk and the associated $\Delta v/v$ value.

have a variation of less than 1 m/sec. The best point for both materials is 45° X, Y and Z cut. The SAW velocity is approximately 1670 m/sec, the power flow angle is zero and the coupling is approximately 0.7×10^{-2} in both the materials. A closer look at the power flow angle at this cut reveals a $\partial\phi/\partial\theta$ value of approximately -0.3. Minimal diffraction requires this to be equal to -1 and low beam steering requires[30] this to be near zero. Hence, this orientation might serve as a compromise between beam steering and diffraction.

Slobodnik et al.[28] have found a minimal diffraction cut in BGO on the 110 cylinder cut, 40.04°. The SAW properties were therefore calculated for BSO for the entire <110> cylinder cut and for the 40.04° cut where the propagation angle was varied in the surface plane. The results, presented in Figure 10 are exactly similar to those obtained for BGO. The minimal diffraction cut which corresponds to $\partial\phi/\partial\theta = -1$ occurs at the same point for BGO and BSO. This cut is 40.04° on the <110> cylinder cut and -90° on the 40.04° cut plotted in Figure 10. Figure 11 presents the SAW and pseudo SAW properties of BSO on the 110 cut. In this cut, a SAW point on the pseudo SAW branch appears at $\theta = -24.5°$ resulting in two SAW velocities for this orientation.

Sulfosalt - Tl_3TaSe_4

Tl_3TaSe_4 along with other members of the ternary thallium chalcogenides family are cubic crystals belonging to the space group R3m. Weinart and Issacs[31] measured the elastic, piezoelectric and dielectric properties of this crystal along with their temperature derivatives. Due to the existence of positive derivatives of the elastic constants, this material might be expected to be temperature compensated. The SAW velocity, coupling, TCD and power flow angles of several cuts are presented in Figure 12. As in BGO and BSO, the cylinder cuts are the 4 row and 2 zero special cases with mechanical motion

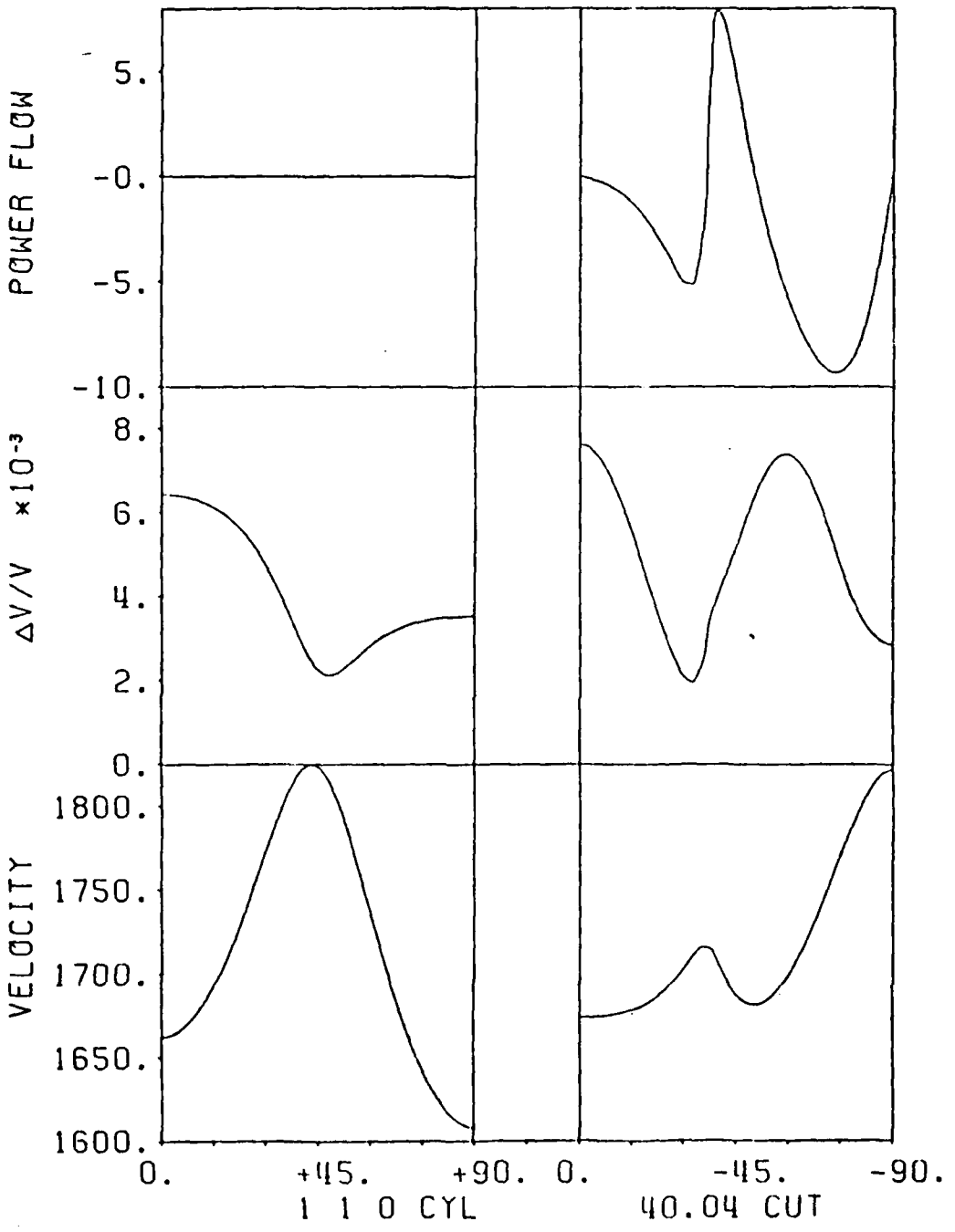

FIG. 10. The variation of the SAW velocity. $\Delta v/v$ and power flow angle for <110> cylinder cut and 40.04° cut R^{90}. The minimal diffraction cut occurs at 40.04° on the <110> cylinder cut and -90° on the 40.04° cut.

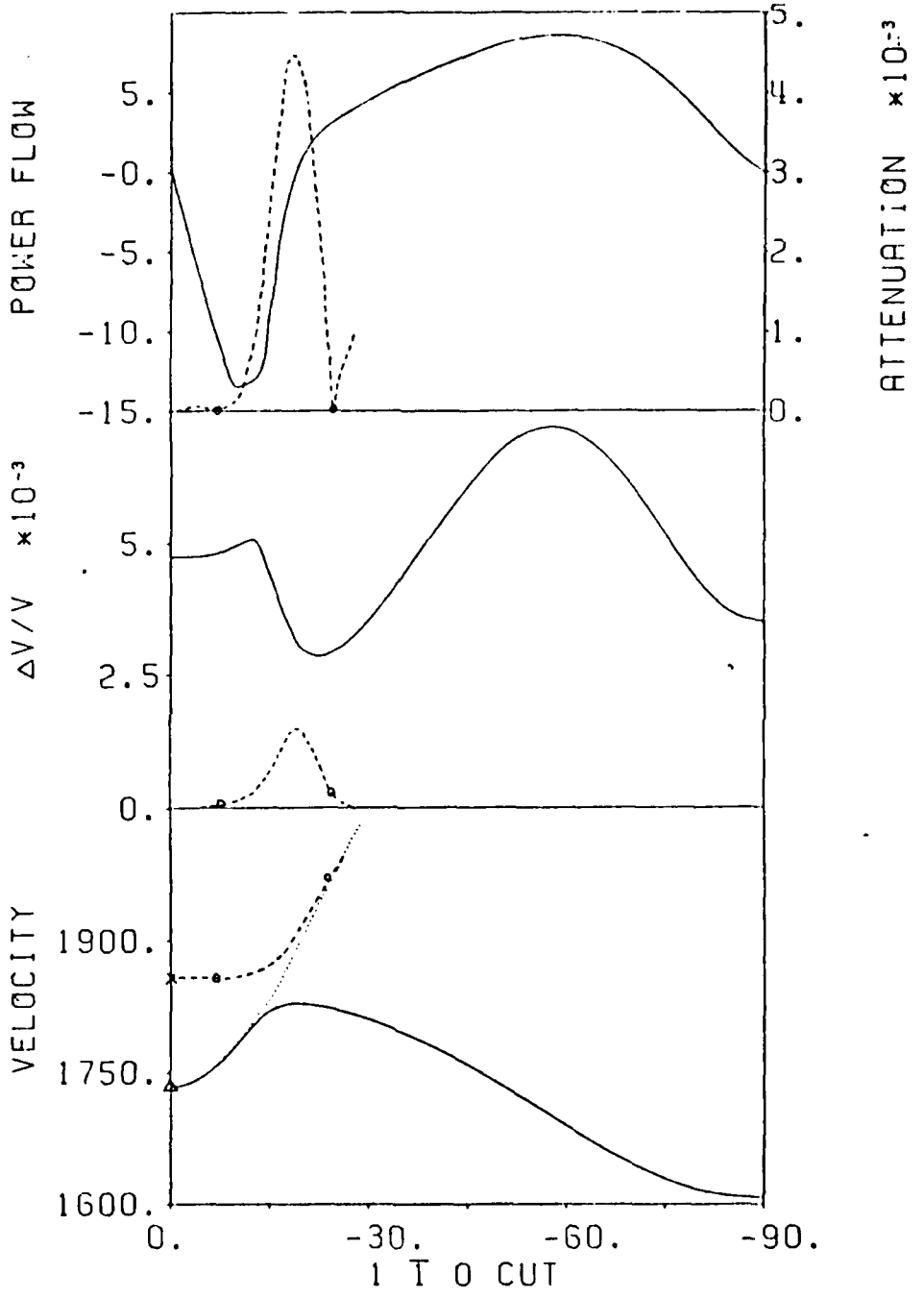

FIG. 11. The variation of the SAW velocity, pseudo SAW velocity, $\Delta v/v$, power flow angle and attenuation factor for the <110> cut in *PZO*. Solid line: properties associated with pseudo-SAW. X: SAW mode with zero coupling. Δ: Bleustein-Gulyaev mode with propagation vector tilted into the bulk and the associated $\Delta v/v$ value. O: isolated SAW points on the pseudo SAW branch and associated properties.

confined to the sagittal plane. The most attractive cut is again the 45° X, Y and Z cut. The SAW velocity at this orientation is 832 m/sec, the coupling is 0.9×10^{-2}, the TCD is -29.4 ppm/°C and the power flow angle is zero. However, the TCD calculations of these cuts do not take into account the temperature variations of the piezoelectric and dielectric constants. Weinart and Issacs[31] included these in their calculations and obtained a temperature compensated cut at 26°, X cut.

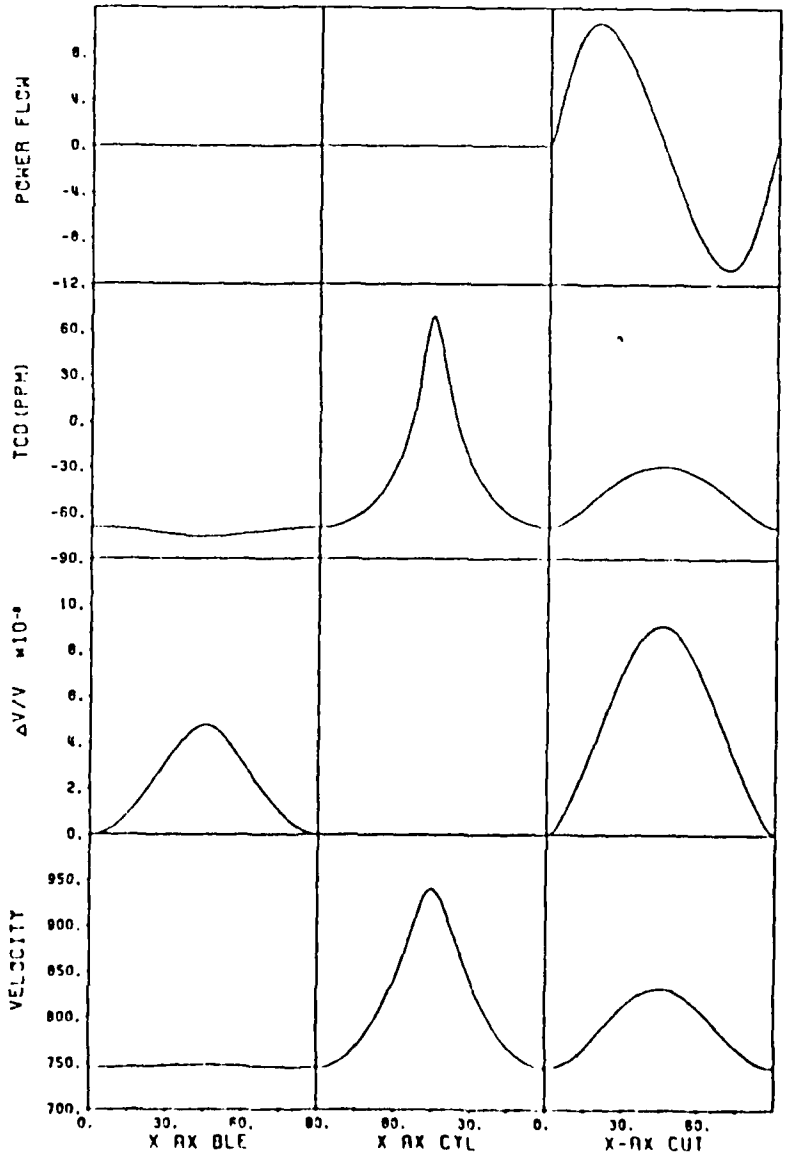

FIG. 12. SAW Properties of Tl_3TaSe_4 for Various Crystallographic Orientations.

Figure 13 presents the SAW and pseudo SAW properties in the <110> cut. Zero degrees in this cut corresponds to 45° of the X, Y and Z cut. Again, at around 15° on this cut a SAW point marked by a circle appears on a pseudo SAW branch. Tl_3TaSe_4 exhibits relatively high coupling and low SAW velocities, however, previous results on temperature compensated cuts revealed high power flow angles. Hence, many crystallographic cuts were searched by the computer

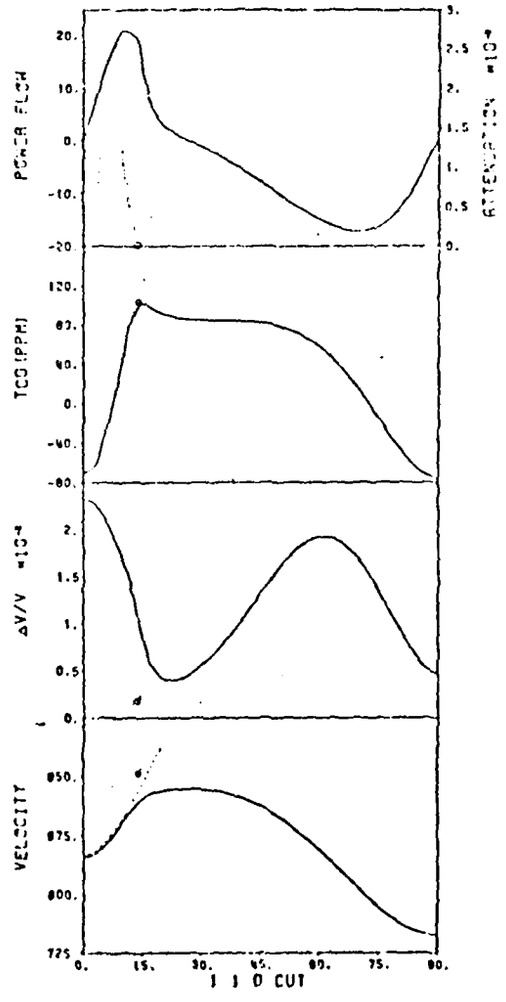

FIG. 13. SAW and Pseudo SAW Properties of Tl_3TaSe_4 for <110> cut. Solid Lines: SAW Properties. Dotted Lines: Pseudo SAW Properties. Dashed Line: Transverse Bulk Velocity. Circle: Isolated SAW Points on Pseudo SAW Branch.

in order to locate ones for which TCD and the power flow angle were simultaneously zero. The <110> axis cylinder cut was found[32] to be such a cut. The variation of the SAW velocity, the electromagnetic to acoustic coupling ($\Delta v/v$), TCD and the lowest bulk velocity for the <110> cylinder cuts in Tl_3TaSe_4 are all presented in Figure 14. The power flow angle is identically zero for the whole cut. This cut is a 1 row 3 zero special case so only 3 roots contribute to the solution. The dotted curve represents the transition velocity where one of the contributing roots moves to the real axis. As is evident from Figure 14, this bulk velocity is quite close to the SAW branch. One might then suppose

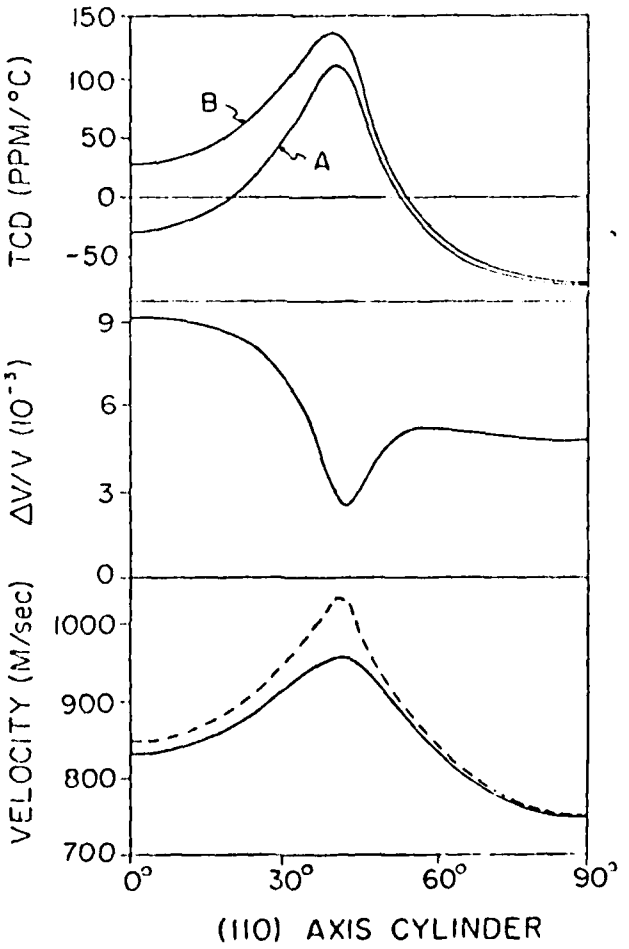

FIG. 14. SAW and Bulk Wave Properties of Tl_3TaSe_4 for <110> Axis Cylinder Cut. Solid Curves: SAW Properties. Dashed Curves: Transverse Bulk Velocity. Curve B Includes Temperature Derivatives of Piezoelectric and Dielectric Constants in TCD Calculations, whereas Curve A does not.

that the depth of penetration of the SAW would be large. However, the term with the highest depth of penetration contributing to the finite coupling mode was found to have a range of penetration depths from about 1.5 to 3 wavelengths for the temperature compensated cuts. The relative contribution of this term to the finite coupling mode was found to be less than 10%. Hence, there seems to be no problem with regard to a deep penetration of the SAW.

The calculations for TCD were performed twice. The data used in calculating curve A did not include the temperature derivatives of the piezoelectric and dielectric constants. The temperature derivatives were used in calculating curve B. However, these derivatives were considered to be only approximate[33]. It is noted that in curve A, two temperature compensated cuts with zero power flow appear while for curve B, only one appears. As the propagation angle increases, the variation between curves A and B decreases indicating that the sensitivity of TCD with respect to the temperature dependence of the piezoelectric and dielectric constants decreases with increasing propagation angle. Therefore, the temperature compensated cut occurring at approximately 54^{o} would be more useful for SAW applications requiring high temperature stability. The piezoelectric coupling for the temperature compensated cuts with zero power flow was roughly one-half that previously reported[31] for temperature compensated cuts in Tl_3TaSe_4. However, the coupling predicted in the present work is still over eight times that in α-quartz. Further, since the power flow angle is zero throughout this cut, the beam steering in the sagittal plane is zero.

Sulfosalts - Tl_3VS_4 and Tl_3TaS_4

Tl_3VS_4 and Tl_3TaS_4 belong to the same family as Tl_3TaSe_4 and are very similar. Issacs *et al.*[31,34] measured their elastic, piezoelectric and dielectric constants and did some preliminary SAW calculations. The results for Tl_3VS_4 are very similar to that of Tl_3TaSe_4. Tl_3VS_4 also has a high coupling

temperature compensated point with a non-zero power flow angle.

A search was instituted on Tl_3VS_4 to try to locate a temperature compensated cut with zero power flow angle. As in the case of Tl_3TaSe_4, this led to the <110> cylinder cut. The SAW velocity, piezoelectric coupling and TCD variations on this cut are plotted in Figure 15. The TCD calculations do not include the temperature variation of the dielectric and piezoelectric constants. The power flow angle is again zero throughout. Approximately 20° and 55° orientations on this cut have a zero TCD and reasonably high coupling. But the inclusion

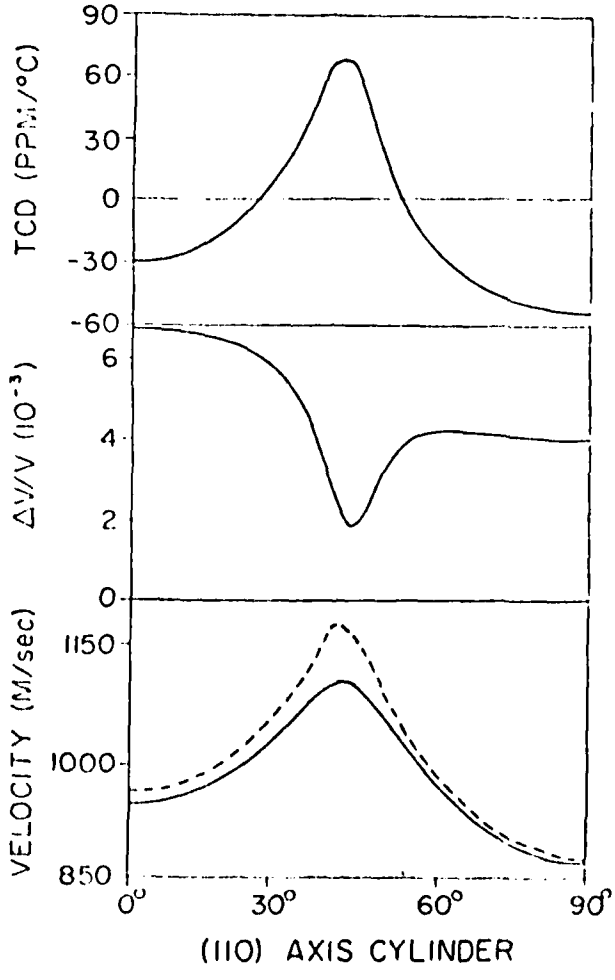

FIG. 15. SAW and Bulk Wave Properties of Tl_3VS_4 for <110> Axis Cylinder Cut. Solid Curves: SAW Properties. Dashed Curves: Transverse Bulk Velocity.

of temperature derivatives of the piezoelectric and dielectric constants in the calculations may change the zero TCD orientations. The dashed curve represents the velocity of transition of one of the three contributing roots to a real root.

Results for the <110> cylinder cut on Tl_3TaS_4 are given in Figure 16. The results are very similar to the other two materials of this family except for the TCD. The TCD values are very high throughout. A few temperature derivatives of this material are opposite in sign to that of Tl_3TaSe_4; this, in all likelihood is a possible explanation for the high TCD.

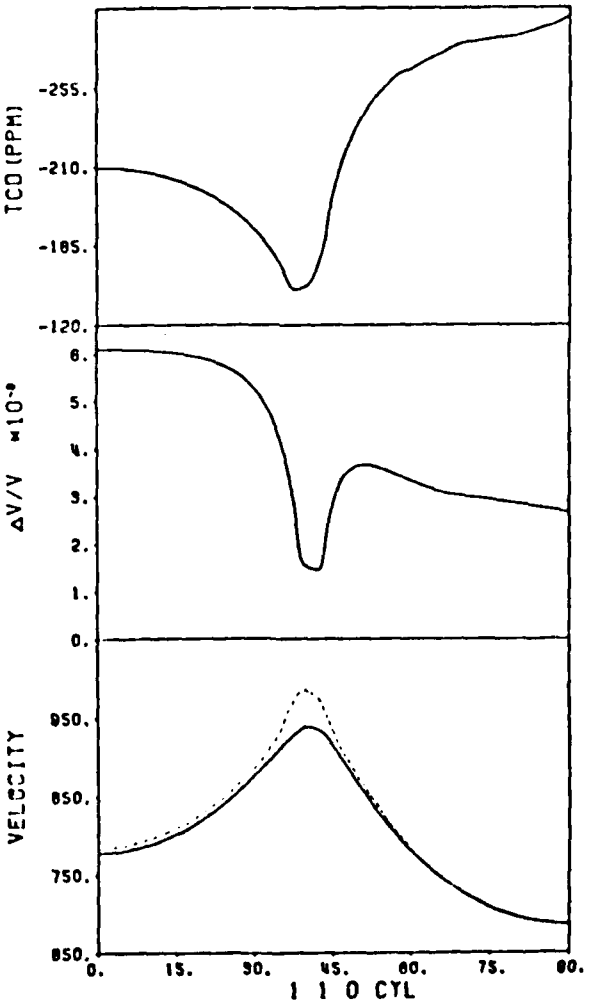

FIG. 16. SAW and Bulk Wave Properties of Tl_3TaS_4 for <110> Axis cylinder Cut. Solid Curves: SAW Properties. Dashed Curves: Transverse Bulk Velocity.

It must be mentioned here, that there are problems with growth of high quality Tl_3TaSe_4, Tl_3VS_4 and Tl_3TaS_4 crystals. These materials will display high losses due to extraneous phases and have relatively sensitive surfaces which distort under normal polishing techniques.

Fresnoite -$Ba_2Si_2TiO_8$

Fresnoite is a new piezoelectric crystal with a noncentro symmetric tetragonal structure, P46m. Growth of single crystals,[35,36] several centimeters long, and measurements of the complete elastic, piezoelectric and dielectric constants have been reported. Due to the existence of a relatively low dielectric constant this material might prove to be useful as a substrate for the silicon air-gap type of SAW convolvers. In fact preliminary calculations indicate that the convolver efficiency, M, is 5-6db higher with fresnoite than with $LiNbO_3$, for the same convolution time and operating frequency.

The SAW velocity, coupling, power flow angle and temperature coefficient of delay were calculated for several orientations and are shown in Figure 17. Due to the symmetry of the fresnoite lattice, all the x and y-type orientations are equivalent. The z-axis cylinder cut is an isotropic cut in that all the SAW properties are the same for this orientation. This cut is identical to the x and y axis boule 0^o orientation.

The SAW velocity and associated properties for the entire x and y axis cylinder cuts and the orientations, z axis boule, 0^o, x and y axis boule, 0^o and x and y axis cut, 0^o and 90^o, can be termed as special cases. In the x and y axis cut, 0^o, orientation, the solution effectively decouples into two solutions. One solution has only two displacement components, one in the direction of propagation and the other perpendicular to the surface. The other solution has a displacement perpendicular to the propagation direction and a scalar potential. The first solution can not be excited

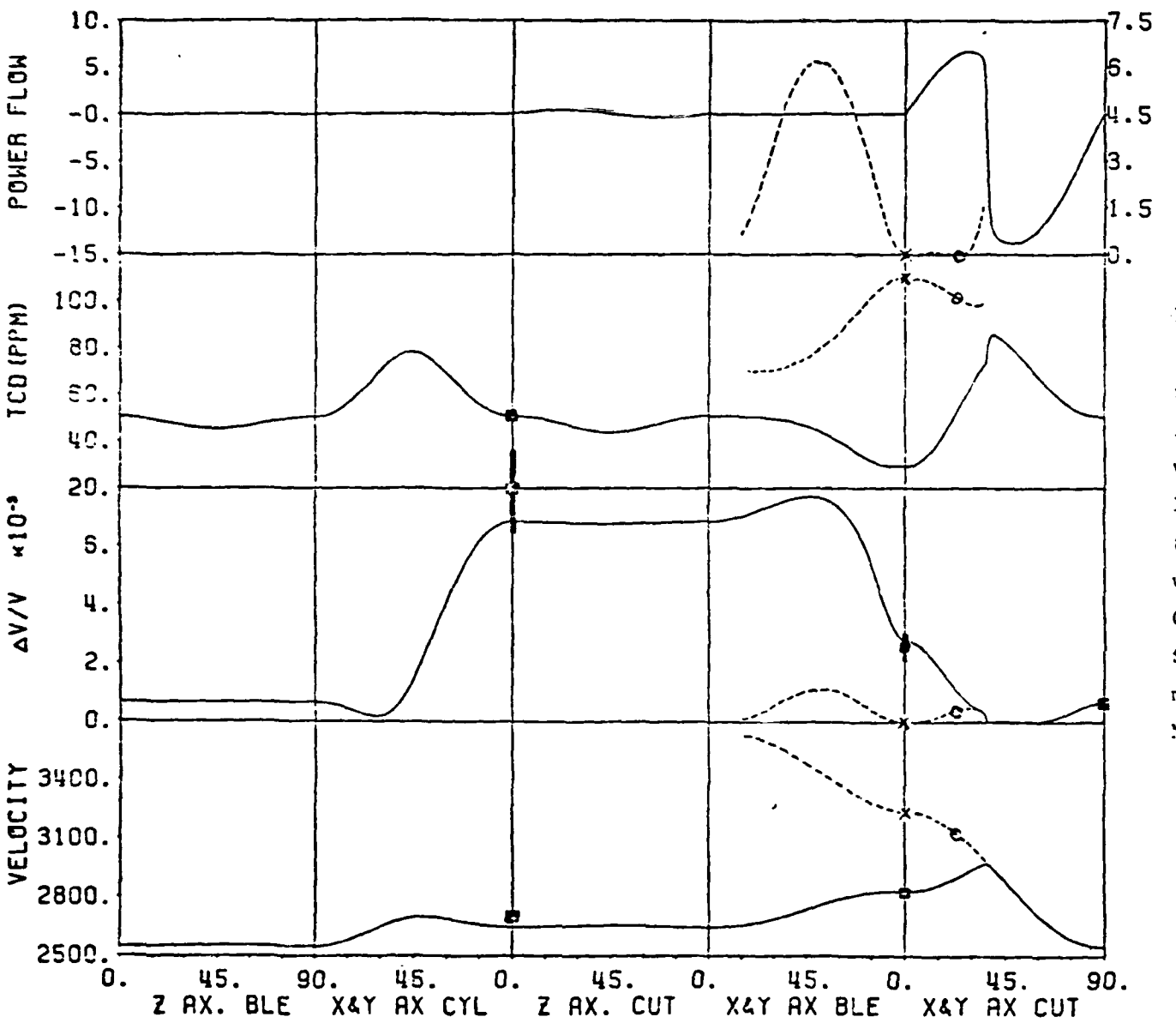

Figure 17. The calculated SAW and pseudo SAW properties of fresnoite. Solid line: Properties associated with the SAW. Dashed line: Properties associated with the pseudo SAW. X, SAW wave with zero coupling. O, isolated SAW on pseudo SAW branch. ■, Experimentally measured points by Melngailis et al.[38]

FRESNOITE

and, hence, has zero coupling, while the latter can be excited and is commonly referred to as a Bleustein-Gulyaev wave. The present calculated results for this point are in agreement with Kimura's calculations[37]. In the other special case orientations the SAW solution has motion only in the sagittal plane and a non zero potential. It is interesting to point out that these special case solutions can exist for both isolated orientations or for entire cuts in fresnoite.

The pseudo SAW velocity and associated properties were also calculated using a computer program developed at the University of Maine. Also shown in Figure 17 is the attenuation associated with this wave. Pseudo SAW solutions were found to exist over part of the x and y axis cuts and x and y axis boule cuts. The point x and y axis cut, 25^{o}, is of special note. The attenuation associated with the pseudo SAW for this orientation becomes zero, hence, rendering two perfect SAW solutions. This type of behavior is similar to that reported by Stegeman[39] in GaAs and Jhunjhunwala et al[40, 41] in berlinite and bismuth silicon oxide. At first glance one is led to the conclusion that the point in the pseudo SAW branch at x and y axis cut, 0^{o}, is also a perfect SAW on a pseudo SAW branch since the attenuation does go to zero. However, this orientation corresponds to the zero coupling solution or non exciteable SAW which has only mechanical displacements associated with it.

An examination of the calculated results and the fact that fresnoite has a low dielectric constant indicates that this material has promise as a useful SAW substrate. The SAW velocities of fresnoite are slightly less than those of $LiTaO_3$ and α-quartz and intermediate between bismuth germanium oxide and $LiNbO_3$. The coupling and temperature stability of fresnoite is comparable

to that of $LiTaO_3$. Fresnoite also exhibits at least one orientation, namely, x and y axis cut, 25°, for which two SAW solutions simultaneously exist. Unfortunately the coupling at this point is quite low. The z axis cut, 45°, and x and y axis boule, 45°, appear to be excellent cuts in terms of reasonable coupling, low diffraction losses and minimal beam steering problems.

Discussion

The most commonly used materials for SAW devices are α-quartz, $LiNbO_3$, $LiTaO_3$ and BGO.[42] α-quartz was the first material used for SAW applications. It possesses several temperature compensated cuts, however, the piezoelectric coupling in this material is quite low. $LiNbO_3$ possessed significantly higher piezoelectric coupling,[27] but the temperature coefficient of delay of this material is high. $LiTaO_3$ was introduced as a compromise material, having more coupling than quartz and a lower temperature coefficient of delay than $LiNbO_3$. BGO[28] is used for long delay lines due primarily to its relatively low SAW velocity. Prior to the onset of this work, other candidate materials which have been investigated include $Ba_2NaNb_5O_{15}$, BGO, CdS, GaAs, InSb, InAs, $LiTaO_3$, α- quartz, TeO_2, ZnO, Lithium Germanate and Tourmaline.

Table 1 lists some general comments about the attractive features and the drawbacks of each of the candidate materials examined in this work. Berlinite, Tl_3TaSe_4 and Tl_3VS_4 were found to be temperature compensated with piezoelectric coupling much higher than quartz. $LiIO_3$ was found to have coupling higher than $LiNbO_3$; and BSO, as far as SAW characteristics are concerned, is a twin material of BGO. Fresnoite with its low relative dielectric constants and reasonable piezoelectric coupling might be a viable substitute for $LiNbO_3$ in convolver applications. In Table 2, a summary of some of the best temperature compensated orientations of the materials examined are presented and compared to materials presently being used. Table 3 compares the coupling of the materials examined to the presently known high coupling materials. Selenium and PKN were found to have coupling even higher than $LiIO_3$, but some uncertainty exists in these results. PKN is also expected to be temperature compensated.

TABLE 1

ATTRACTIVE FEATURES AND DRAWBACKS
OF THE MATERIALS EXAMINED

MATERIAL	ATTRACTIVE PROPERTIES	POSSIBLE DRAWBACKS
$LiIO_3$	1. High Coupling 2. Moderate SAW Velocity	1. High TCD 2. Slightly hygroscopic
α-HIO_3	1. Low SAW Velocity	1. High TCD 2. Moderate coupling 3. Hygroscopic
Berlinite	1. Temperature compensated cuts 2. Moderate coupling 3. Pure mode axes	1. Large enough single crystals not available 2. Experimental verification required
Selenium	1. High coupling 2. Very low SAW Velocity	1. Uncertainty in data 2. Poisonous
PKN	1. High coupling 2. *Possibly Temperature* compensated	1. Large enough single crystals not available
BSO	1. Low SAW Velocity 2. Minimal diffraction cut	1. Temperature derivative data not available
Tl_3TaSe_4, Tl_3VS_4	1. Very low SAW Velocities 2. Temperature compensated cuts 3. Moderately high coupling 4. Pure mode axes	1. Soft material, high loss
Tl_3TaS_4	1. Very low SAW Velocity 2. Moderately high coupling	1. High TCD (uncertainty) 2. Soft material, high loss
$Ba_2Si_2TiO_8$	1. Very low dielectric constants 2. Reasonable piezoelectric coupling	1. Large single crystals are not currently available

TABLE 2

TEMPERATURE COMPENSATED MATERIALS

MATERIAL	CRYSTALLOGRAPHIC ORIENTATION	SAW VELOCITY (M/sec)	$\Delta v/v$ (10^{-2})	POWER FLOW ANGLE (deg)
α-$AlPO_4$[a]	x cut 22°	2751	0.20	-.55
	y cut 6.8°	2749	.221	4.5
	x axis Ble. 37°	2855	.015	0.0
	92.75°	2733	.220	0.0
	z cut 84°, 36°, 24°	3090	.117	16.5
	y axis Ble. 65.5°	2865	.277	-2.9
	9.5°	3113	.162	10.0
α-quartz[b]	x cut 33.5°	3180.	.033	5.0
	-29°	3620.	.035	-12.0
	y cut 36°	3360.	.04	3.5
	-36°	3360.	.04	-3.5
	z cut 0°, 60°	3260.	.006	0.0
	ST cut 0°	3160.	.0058	0.0
	46°	3330.	.0035	10.5
	-46°	3330.	.0035	-10.5
TeO_2[b]	x and y cut 39°	1424.	.008	37.5
	-39°	1424.	.008	-37.5
	x and y axis Ble. 58.2°, -58.2°	1387.	.0002	0.0
Tl_3VS_4[c] (a)	(110) cut, 70°	900.	1.0	-17.0
	(110) cyl, 24°	1010.	.617	0.0
	53°	1033.	0.4	0.0
Tl_3TaSe_4[d] (a)	x cut 26°	800.	1.2	12.8
	(110) cut 75°	790.	1.4	18.0
	(110) cyl 19°	865.	.85	0.0
	53°	889.	.496	0.0

[a] Present work

[b] Ref. (3): Result read from curves

[c] Ref. (31): Result read from curves

[d] Ref. (34): Result read from curves

TABLE 3

HIGH PIEZOELECTRIC COUPLING MATERIALS

MATERIAL	MAXIMUM $\Delta v/v_2$ ($x10^{-2}$)	MINIMUM velocity (M/sec)	MAXIMUM velocity (M/sec)	MINIMUM TCD(ppm/^{o}C)
$LiNbO_3$[b]	2.8	3318	4000	72
$LiIO_3$[a]	4.34	1904	2258	260
$LiTaO_3$[b]	0.87	3110	3390	24
BGO)*,[a]	0.80	1623	1834	---
BSO)	0.76	1607	1855	---
$Ba_2Si_2TiO_8$	.76	2550	2980	32

Selenium and PKN have been found to possess a coupling higher than $LiIO_3$.

[a] Present Work

[b] Ref. (3)

*Material Possesses minimal diffraction cuts

C. Layered Media

Theory and modes

A composite SAW structure consisting of a layer over a substrate has, in many cases, SAW properties which might be very useful in an actual device. High velocity composite structures[43] which would enable one to go to high frequencies and high coupling temperature stable composite structures[44-46] have been the subject of some experimental investigations. In spite of the attractiveness of composite structures, one should note that material preparation and fabrication problems are more involved in these structures. Due to the fact that experimentally and theoretically proven single crystal substrates which combine several attractive SAW properties such as high coupling and temperature compensation are at present not available, a theoretical study of the modes in various composite structures was undertaken. The resulting computer program is of course more complicated than the corresponding work in a single crystal.

A theoretical study of the various acoustic modes and associated properties were made on all combinations of a piezoelectric or nonpiezoelectric layer and a piezoelectric or nonpiezoelectric substrate. The program also took into account any conductivity or viscosity which might be associated with the layer or substrate. Arbitrary orientations of the layer and the substrate were allowed. The acoustic wave velocities, piezoelectric coupling ($\Delta v/v$), temperature coefficient of velocity (TVC) and the power flow angle were calculated as a function of layer thickness.

Depending upon the isotropy or anisotropy of both the layer and substrate various types of acoustic modes can occur. When both layer and substrate are isotropic, the acoustic wave can be of two types. One wave is a Love wave with particle motion perpendicular to the sagittal plane. This wave can exist only if the transverse shear velocity of the layer is less than that of the surface

wave. The Love modes can be infinite in number. The other type of surface wave in this structure is a Rayleigh wave with particle motion confined in the sagittal plane. If the layer shear velocity is not much less than the substrate shear velocity, only a single mode will occur. At zero layer thickness, this mode corresponds to the substrate Rayleigh wave. The velocity of the mode increases with layer thickness until it is equal to the substrate shear wave velocity at some critical layer thickness. However, if the layer shear velocity is much less than the substrate shear velocity, than a large number of modes are possible.

If either the substrate or the layer or both are anisotropic, the situation is more complex. In general, the waves can not be divided into Rayleigh or Love modes though in many cases, the particle motion can still be predominantly in the sagittal plane or perpendicular to it.

In a single piezoelectric or nonpiezoelectric substrate, the solution for the SAW can be one of five types. In a nonpiezoelectric substrate the following two types are possible: (i) a solution with displacements μ_1, μ_2, and μ_3, and (ii) solutions with either μ_1 and μ_3 or μ_2 alone. In a piezoelectric substrate, the following three type are possible: (i) a solution with μ_1, μ_2, μ_3 and ϕ, (ii) solutions with either μ_1 and μ_3 or with μ_2 and ϕ (this case is commonly called the 4 row 2 zero case, the latter solution being the Bleustein-Gulyaev wave) and (iii) solutions with either μ_2 or μ_1, μ_3 and ϕ (this case is commonly called the 1 row 3 zero case). Any one of these five solutions in a substrate can be combined with a likewise combination of solutions in the layer. Furthermore, the geometry can include a thin mass less metallic plate at the surface of the layer, at the interface, both at interface and surface, or at neither the surface nor interface. These combinations give rise to a large number of forms of the boundary condition matrix. These combinations have been

grouped into thirteen different cases, each of which has to be handled in a different manner. A computer program has been written to handle all these thirteen cases. It calculates velocity, coupling, TCV and power flow angle for any symmetry layer or substrate and with or without the massless metallic plates at any of the surfaces.

Plate Modes

If one allows the substrate thickness to vanish and considers the layer to be piezoelectric, one can obtain the plate modes. Plate modes in a piezoelectric layer are analogous to those occurring in a dielectric layer wave guide in that they are discrete and have appropriate cut off frequencies. A computer program was developed to calculate the plate mode spectrum given the thickness in wavelengths.

This work in plate modes was motivated in part by a recent experimental measurement by Carr[47] on Z-cut x propagating $LiNbO_3$. A new low-loss high coupling mode whose velocity was above that of the ordinary Rayleigh type SAW mode was observed in this cut. This mode also exhibited less insertion loss than the SAW. The experimentally observed velocity of this mode was in excellent agreement with the theoretically calculated metallized pseudo SAW velocity. However, a theoretical analysis showed that the attenuation of the pseudo SAW was so high that it lost half of its energy in a distance shorter than the interdigital transducer length. It was then decided to calculate the plate mode spectrum. This calculation is shown in Figure 18 for 1 mm thick 1.4μ line width transducer on ZX $LiNbO_3$. Due to the large thickness of the plate in wavelengths, there were a large number of allowed plate modes very close to one another. The plate mode coupling however, peaks at approximately the same point as the pseudo SAW. Further experimental measurements by Carr[47] showed that the output transducer location was critical thereby giving credulence to the

idea that this new mode was reflected from the bottom. It is theorized that the presence of the pseudo SAW enhances the normal volume wave radiation. This causes the plate mode spectrum to have a coupling peak at approximately the pseudo SAW velocity. Since the coupling peak for the individual plate modes is not as high as the experimentally observed coupling of the volume modes, one is led to the conclusion that the energy radiated from the pseudo SAW goes into more than one plate mode. Further calculations have shown that the coupling to volume modes of much thinner plates to be greater than that of the SAW. Also, it has been noted that this high coupling volume mode or combination of plate modes seems to occur whenever a pseudo SAW solution is allowed. A potential application of this volume wave mode is in low-loss broad-band signal processing devices.

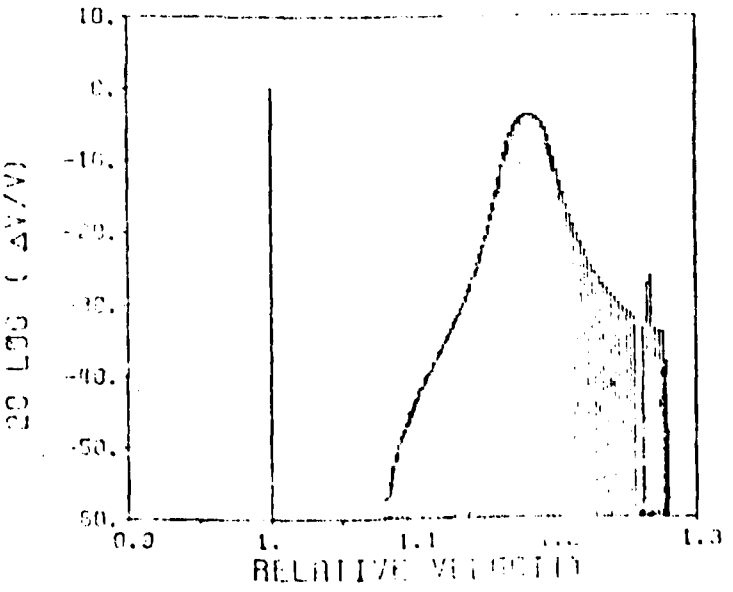

FIG. 18 Plate modes for 1 mm thick ZX $LiNbO_3$ plate with 1.4 μm line width and operating at 398 MHz. 1 on the horizontal scale and 0 db on the vertical scale corresponds to SAW velocity and coupling.

Experiment

In order to characterize the effect of a layer on the SAW properties, measurements of the SAW velocities and temperature coefficients of delay (TCD) were made as functions of layer material and thickness.

Initially, the delay line was fabricated using standard photolithographic techniques. Deposition of the metal film overlay was done in a high vacuum system at pressures ranging from 10^{-6} to 10^{-8} torr. The vacuum system incorporates an electron beam for evaporating the layer material on the sample. The system also incorporated a crystal ocsillator to provide continuous monitoring of the deposition rate and thickness of the deposited layer. In order to prevent deposition on the transducers, metal shields are used to mask the transducers. A deposition rate of about 10Å/sec or less produced a layer with fairly uniform thickness. In order to maximize the electrical power coupled in and out of the SAW delay line, the transducers were electrically matched at the center frequency. The center frequency of the transducers were easily measured by the single transducer technique[48], where the equivalent shunt conductance as a function of frequency of each transducer is measured using a bridge. The frequency corresponding to the peak value of the conductance is the center frequency. Measurements were often affected by the presence of external electromagnetic fields, hence the device was mounted in a metal case. The velocity was measured using the impulse response technique[48]. The temperature coefficient of delay was measured using the oscillator technique[48].

Results

The SAW substrates chosen for study were $LiNbO_3$ and $LiTaO_3$. The overlays used were gold, silver, copper, chromium, aluminum, cadium sulfide and fused quartz. The above metals were selected for two reasons. First, they represent

a wide range in density, from 2.7 $g/_{cm}3$ (aluminum) to 19.32 $g/_{cm}^{3}$ (gold). Hence the effect of density on the various SAW properties can be studied. Second, these metals are among the best electrical conductors, therefore, the losses due to electrical conductivity were anticipated to be small.

Except for a few cases, results are presented under three different categories. These are, the variation of the fractional delay change ($\Delta\tau/\tau$) as a function of temperature for various overlay thicknesses; the variation of the SAW velocity at 25°C as a function of overlay thickness; and the variation of the overlay thickness necessary to achieve temperature compensation as a function of the compensation temperature. The quantity h.k referred to as overlay thickness in the various graphs, represents the overlay thickness (h) multiplied by the wave number (k).

Overlays on Quartz Substrates

The theoretical results have been obtained for the ST, AT and YX cuts in quartz with gold, silver, copper, chromium and CdS overlays. Examples of experimental and theoretical results obtained for various overlays on quartz substrates are presented in Figures 19-21. The maximum overlay thicknesses used on the ST, AT and YX cuts in quartz were 0.004, 0.015 and 0.1 wavelengths respectively. The theoretical calculations were performed at a frequency of 40MHZ and in a temperature range between 0°C and 50°C.

The experimental results presented include aluminum and gold overlays on ST cut quartz and gold overlays on YX cut quartz. For aluminum overlays on ST quartz, the thickness of the overlays used were 1.6×10^{-3} and 3.2×10^{-3} wavelengths. For gold overlays on ST quartz, the thicknesses used were 1.6×10^{-4}, 3.2×10^{-4} and 4.8×10^{-4} wavelengths. The thickness of the gold overlay used on YX quartz was roughly 0.14 wavelengths. The SAW delay lines used were fabricated to operate at a center frequency of roughly 40MHZ. The relatively large thickness of the gold overlay required on YX quartz caused

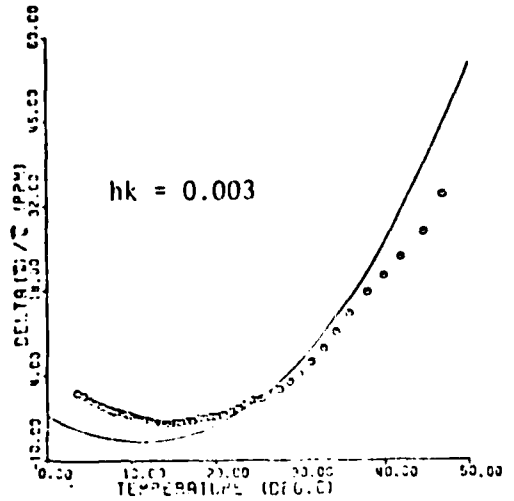

Fig. 19a

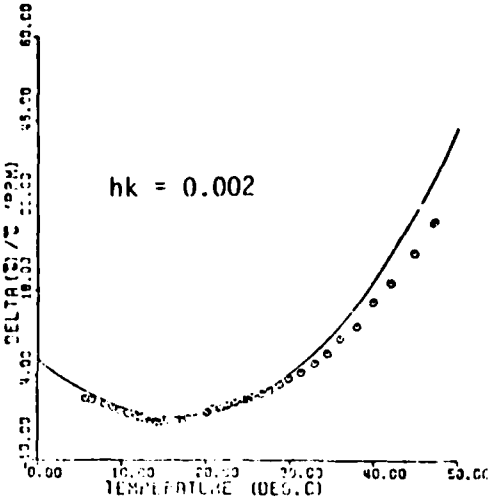

Fig. 19b

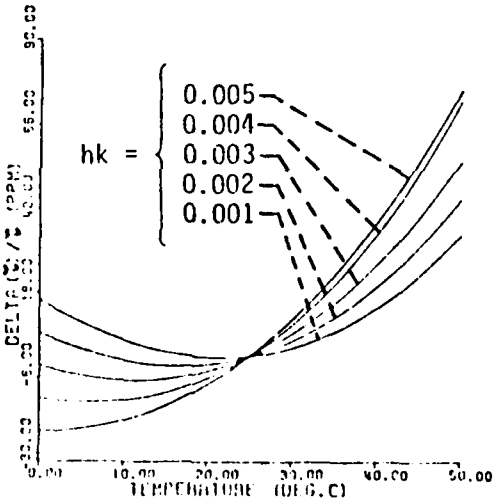

Fig. 19c

Fig. 19 Gold Overlay on ST Quartz. Solid Lines-Theory, Circles-Experiment. a) $\Delta f/f$ Versus Temperature for hk = 0.003. b) $\Delta f/f$ Versus Temperature for hk = 0.002. c) $\Delta f/f$ Versus Temperature for Various Overlay Thicknesses. (Figures Continued)

Fig. 19 (Continued)

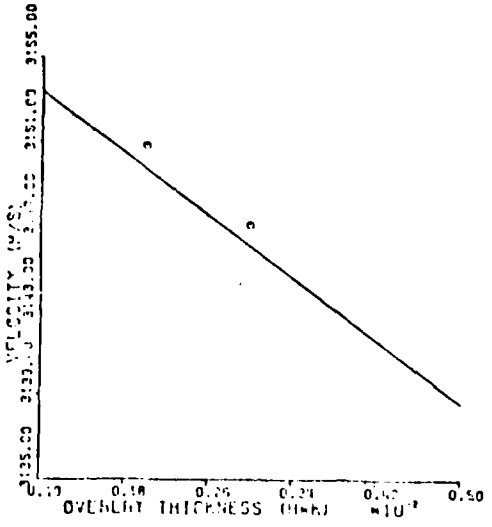

Fig. 19d

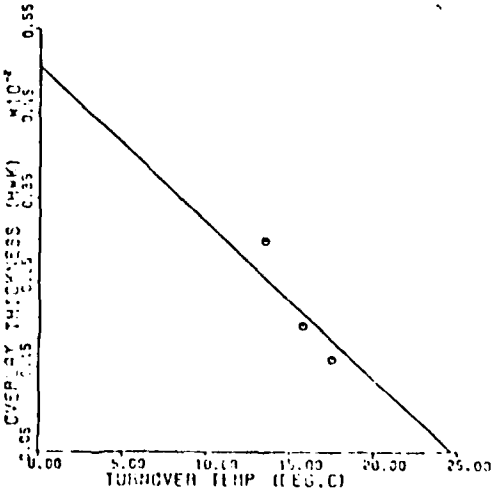

Fig. 19e

d) Velocity Versus Overlay Thickness at 25°c.
e) Overlay Thickness Versus Turnover Temperature.

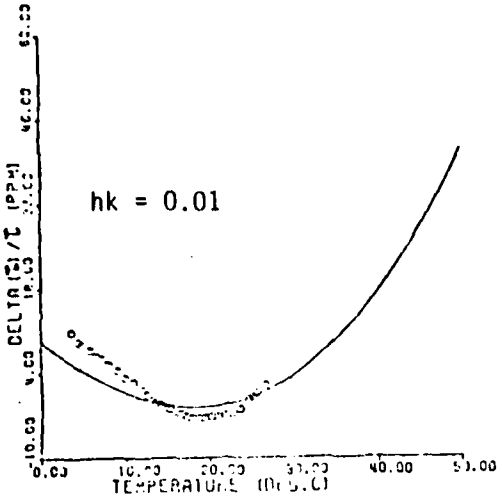

Fig. 20a

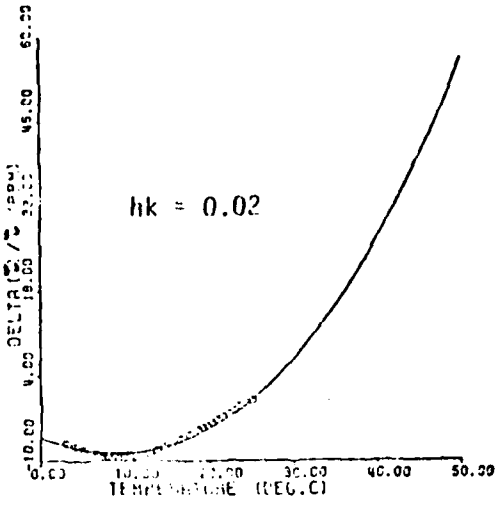

Fig. 20b

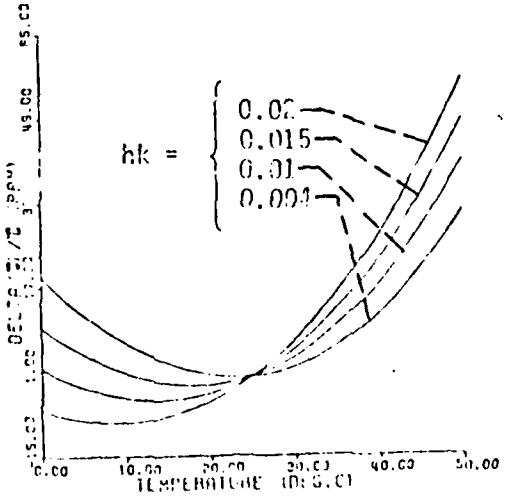

Fig. 20c

Fig. 20 Aluminum on ST Quartz. Solid Lines-Theory, Circles-Experiment. a) $\Delta f/f_1$ Versus Temperature for hk = 0.01. b) $\Delta f/f_1$ Versus Temperature for hk = 0.02. c) $\Delta f/f_1$ Versus Temperature for Various Overlay Thicknesses.
(Figures Continued)

Fig. 20 (continued)

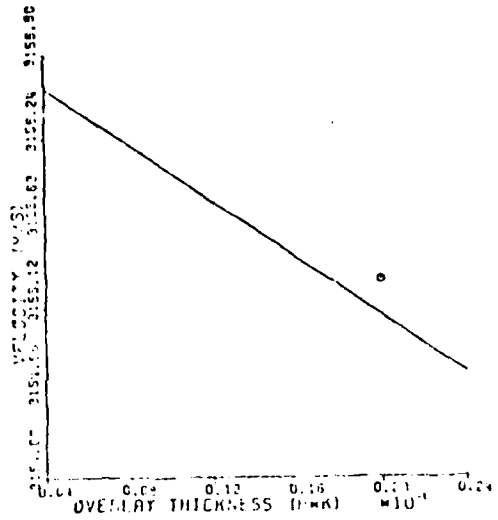

Fig. 20d

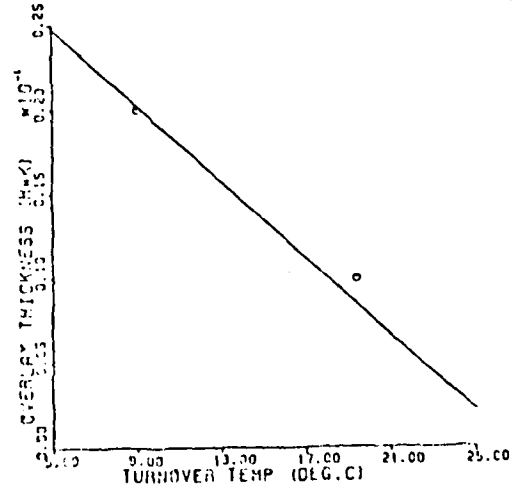

Fig. 20e

d) Velocity versus Overlay Thickness at 25°C.
e) Overlay Thickness versus
Turnover Temperature.

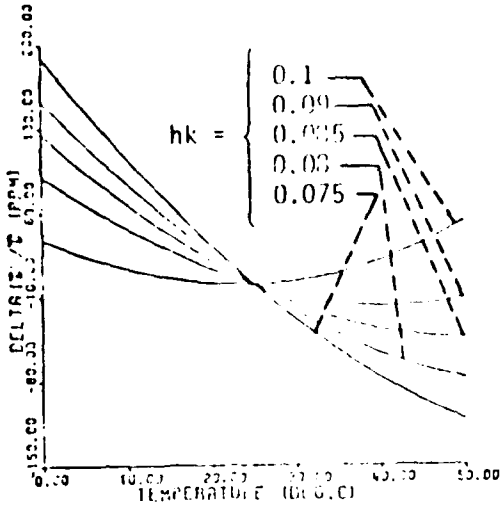

Fig. 21a

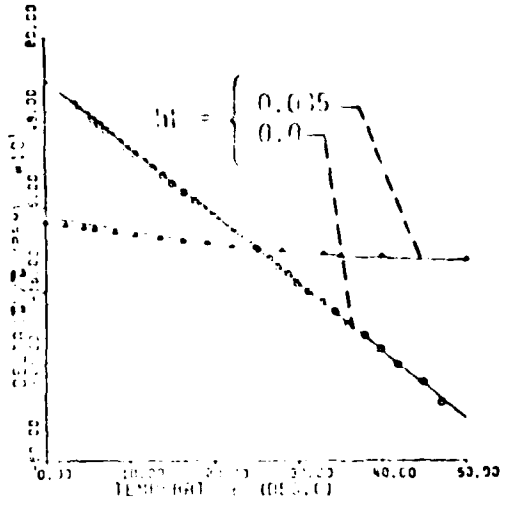

Fig. 21b

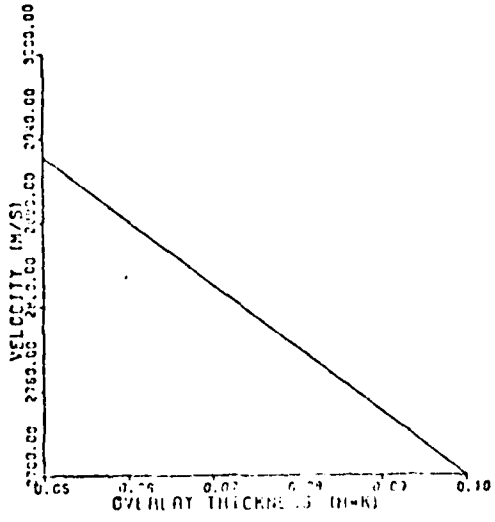

Fig. 21c

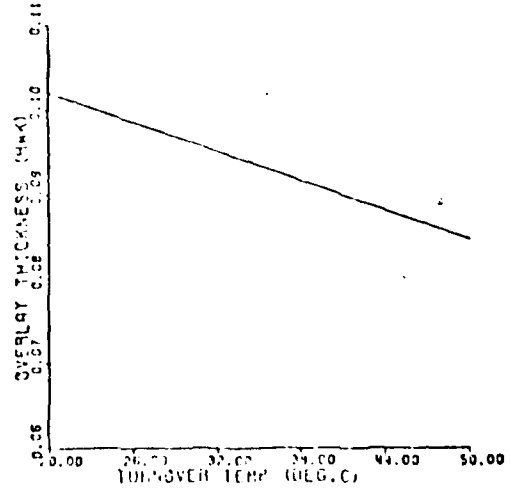

Fig. 21d

Fig. 21 Cold Overlay on YX quartz, Solid lines-Theory, circles and triangles-experiment. a) $\Delta t/t$ versus Temperature for Various Overlay Thickness. b) $\Delta t/t$ versus Temperature for hk = 0 and hk = 0.035. c) Velocity versus Overlay Thickness at 25°C. d) Overlay Thickness versus Turnover Temperature.

difficulties during overlay deposition. Hence only one deposition could be made on YX quartz. This meant that the SAW velocity measurements could not be made for different thicknesses of the overlay.

Overlays on $LiNbO_3$ and $LiTaO_3$ Substrates

The theoretical results for the variation of the fractional delay change as a function of temperature for gold, aluminum and fused quartz overlays on various cuts in $LiNbO_3$ and $LiTaO_3$ were obtained. The calculations were performed at a center frequency of 40MHZ.

For these two substrates the most promising results obtained were for the fused quartz layer on to 41.5° rotated x propagating cut of $LiNbO_3$. For a $\lambda/4$ wavelength thick fused quartz layer and the transducer at the layer-substrate interface, the acoustic wave has a zero TCV, a velocity of around 4000 m/sec, piezoelectric coupling above 0.06 and a zero power flow angle. This coupling is much higher than that obtained on single crystal $LiNbO_3$. In general, this composite structure was characterized by high coupling and temperature compensation.

Discussion and Conclusions

Most of the results obtained for the variation of the SAW velocity as a function of overlay thickness can be classified into two categories. In the first category, the SAW velocity decreases linearly with increasing overlay thickness, hk. In the second, the SAW velocity increases linearly with increasing overlay thickness. All overlay structures fall into the first category with the exception of the chromium overlay on ST quartz and the aluminum overlay on YX quartz. The chromium overlay on ST quartz belongs to the second category. The SAW velocity for the aluminum overlay on YX quartz does not fall into either of the two categories. In this case the SAW velocity

exhibits a parabolic behaviour with increasing thickness and reaches a minimum at a thickness of hk = 0.3.

In order to explain the variation of the SAW velocity as a function of overlay type and thickness, one must examine the value of the Rayleigh wave velocity in the overlay alone and in the substrate alone. If the Rayleigh wave velocity in the overlay is much less than the corresponding velocity in the substrate, the SAW velocity in the composite structure tends to decrease with increasing overlay thickness. The SAW velocity is approximately equal to the Rayleigh wave velocity of the substrate for small overlay thicknesses and decreases steadily as the thickness is increased, until the velocity becomes asymptotic to the Rayleigh wave velocity in the overlay. This usually occurs for overlay thicknesses on the order of a few wavelengths. The overlay is said to load the substrate in this case. If the Rayleigh wave velocity in the layer is considerably higher than the corresponding velocity in the substrate, the velocity in the composite increases with increasing overlay thickness. The velocity is close to the Rayleigh wave velocity in the substrate for small overlay thicknesses and becomes asymptotic to the Rayleigh wave velocity in the overlay for overlay thicknesses in the order of a few wavelengths. In this case the overlay is said to stiffen the substrate. When the Rayleigh wave velocities in the substrate and the overlay are close to one another, the variation of the SAW velocity in the composite as a function of overlay thickness is more complicated and depends on such factors as the loading or stiffening effect of the overlay, the relative values of the shear wave velocity in the layer and the Rayleigh wave velocity in the substrate. In general, one may say that the velocity in the composite is close to the Rayleigh wave velocity in the substrate for small overlay thicknesses and is close to the Rayleigh wave velocity in the overlay for relatively large overlay thicknesses.

The use of gold, silver, copper and CdS overlays on quartz was found to decrease the SAW velocity with increasing thickness. Use of chromium overlays on ST quartz however increased the SAW velocity with increasing overlay thickness. In order to understand these results, it is necessary to compare the Rayleigh wave velocities in the substrate and overlay for each case. The Rayleigh wave velocities in ST, AT, and YX quartz range between 3150.0 and 3160.0 m/s. The shear wave velocity in gold, silver, copper and CdS are 1485.0, 2060.0, 2900.0 and 1750.0 m/s respectively. The Rayleigh wave velocity in each material is always less than the corresponding shear wave velocity. Hence the Rayleigh wave velocities in gold, silver, copper and CdS are considerably less than the corresponding velocity in quartz. The use of these overlays on quartz therefore causes the velocity to decrease with increasing thickness, due to the loading effect. In the case of chromium the shear wave velocity is 3761.1 m/s therefore the Rayleigh wave velocity in chromium is higher than the corresponding value in ST quartz. Chromium overlays therefore produced a stiffening effect on the quartz substrate, causing the velocity to increase with increasing overlay thickness.

The use of aluminum overlays on ST and AT quartz was found to decrease the velocity with increasing overlay thickness. In the case of aluminum on YX quartz, the velocity varied in a parabolic fashion, reaching a minimum at hk = 0.3. The shear wave velocity in aluminum is 3220.0 m/s and is higher than the Rayleigh wave velocity in YX quartz. The Rayleigh wave velocity in aluminum however is 2941.0 m/s and is lower than the corresponding velocity in YX quartz. For small thicknesses of aluminum overlay on ST, AT and YX quartz, the SAW velocity decreased with increasing thickness. For relatively larger overlay thicknesses, the effect of the nigher shear wave velocity in the layer causes the

velocity in the composite to increase with an increase in thickness. The shear wave in the overlay, cannot however be sustained for larger thicknesses as it requires considerably more energy than the Rayleigh wave. The velocity is therefore expected to decrease again after a certain value of overlay thickness and reach the Rayleigh wave velocity in the overlay for large overlay thickness. This sort of behavior has not been reported in any overlay - substrate geometry.

It has been observed in both the theoretical calculations and experimental work that the turnover temperature decreases linearly with increasing layer thickness, hk, for all cases studied. In order to explain this behavior it is necessary to consider why the overlay causes temperature compensation. Details relating to this are given elsewhere [49].

The agreement between the theoretical and experimental results for $\Delta\tau/\tau$ as a function of temperature have been found to be good for gold overlays on YX quartz and aluminum overlays on ST quartz. The agreement is fair in the case of gold overlays on ST quartz. The thickness of the overlays used in the latter case is an order of magnitude smaller than those used in the former case. This is thought to be one of the main reasons for the fair agreement in the case of gold overlays on ST quartz. In the theoretical calculation performed the various elastic constants used for the overlay were actually the bulk constants for the overlay material. It is thought however that the elastic constants for thin films differ from the corresponding elastic constants for the bulk. The better agreement observed between the two results for thicker overlays justifies this claim. Additional error could have resulted from the non-uniform thickness of the overlays used in the experiment.

The present work has shown that the use of metallic and semiconductor overlays on various cuts of quartz, $LiTaO_3$ and $LiNbO_3$ as a means of improving the

temperature characteristics and also providing temperature compensation is possible. For overlays which produce a loading effect on the substrate, the use of heavier overlays have been found to decrease the SAW velocity considerably more than the lighter overlays for a given thickness. An overlay with positive TCD in combination with a substrate with negative TCD and vice-versa are found to cause temperature compensation in the composite structure. The slope of the thickness versus turnover temperature curve is found to be always negative and linear for small thicknesses. The slope is small in magnitude when heavier overlays are used. For larger overlay thicknesses the slope is found to increase with increasing thickness. Some of these factors such as slope of the dispersion curve, the overlay thickness required to temperature compensate a given substrate at room temperature and the degree of improvement in the temperature characteristics can be used as a guide for selecting an appropriate overlay for device application.

D. Diffraction

Theoretical and experimental work was performed in order to obtain the diffraction profiles of a large number of crystals. These profiles are considered to be a very important SAW property with regard to the suitability of a SAW substrate for device application. This section summarizes some of the significant accomplishments in the area of SAW diffraction.

Theory

Three computer programs were written for performing diffraction calculations. One was based on the parabolic theory. The program was very similar to the one written by Szabo and Slobodnik[30] and assumes a parabolic velocity profile. Loss calculations were also done. The second program was based on the angular spectrum of waves approach without the use of an FFT alogrithom. The program was

again similar to the one used by Szabo and Slobodnik[30] with some differences. In this program, double precision was required in the calculation of a phase term in the integrand. Hence, to conserve memory and to save time, only the phase term was evaluated in double precision. Another difference was in the steps involved in the evaluation of the integrand. The intermediary steps were such that less time was required for this calculation. Further, to conserve memory, none of the intermediary variables were defined in terms of an array. Instead, dummy variables were used which could be used repeatedly in the program.

The overall effect of these changes was a considerable economy in the memory used and the execution time. However, the time required for the calculation of diffraction profiles was still extremely large and the program was not suitable for frequent utilization by SAW designers. The third program makes use of a fast Fourier transform algorithm to considerably reduce the time required to theoretically evaluate a diffraction profile.

The first part of the program which makes a velocity table (K_1 vs. K_3 table) was the same as the one used for the previous program. A common choice for the number of points in this table was 2^9, although provisions were made for varying it. Three point interpolation was used to find the intermediate velocity points. Then a forward fast transform was performed to obtain the intensity profile. Intensity and loss calculations were then obtained easily and quickly.

These modifications made it possible to calculate diffraction profiles about 60 times faster than by the program reported by Szabo and Slobodnik[30]. A typical calculation on our IBM 370-145 using a Fortran H compiler required 22 seconds for the first profile and 15 seconds for each succeeding profile. The points obtained were $\lambda/2$ apart in the X direction and include the time

required for the output and loss calculations. The time required for different X increments is given in Table 4. The details of this program is presented elsewhere[50].

Using the third program described above, diffraction profiles were calculated for berlinite (α-$AlPO_4$), TeO_2, α-quartz, Tl_3VS_4, and Tl_3TaSe_4. In particular, the temperature compensated cuts of these materials were investigated. The particular cuts investigated and related SAW data are presented in Table 4. Only the results for cuts having a zero power flow angle and a reasonable coupling will be presented here. The complete results may be found in reference 50.

Profiles for berlinite X-cut boule 37^o and 92.75^o are presented in Figures 22 and 23 respectively for 5 different distances from the transducer. The diffraction losses of each of these profiles is also presented. Z is the distance from the transducer in wavelengths and X (O) is the distance, in wavelengths, from the propagation axis to the center of the profile. Similar results are presented in Figures 24 and 25 for α-quartz, Z-cut 0^o and ST-cut 0^o respectively.

The 37^o X-axis boule cut for berlinite has a very high diffraction loss compared to the 92.75^o cut. This, together with a much higher coupling, indicates that the 92.75^o X-axis boule cut of berlinite is the most suitable for device applications. Similarly, the 0^o ST-cut of α-quartz appears to make it the most suitable cut because its lower diffraction loss offsets its slightly lower coupling.

Experiment

An experimental diffraction profile study was not included in our proposal of work to be undertaken under this contract. However, since it would be a very useful adjunct to our theoretical work it is briefly mentioned here. It should be stressed that the necessary equipment was purchased by the

TABLE 4.

BREAKDOWN OF TIME REQUIRED FOR THE DIFFRACTION PROGRAM
USING FFT (ALL TIMES ARE APPROXIMATE)

X Separation ΔX	Number of points in the velocity table $K_{max}/\Delta K$	Order of FFT N	Time for velocity table (sec)	Time for calculation of integrand (sec)	FFT time (sec)	Output and loss (sec)	Total Time for first beam profile calculation (sec)	Total Time for succeeding beam profile calculation (sec)
λ	2^9	2^{11}	6	3.6	3.4	4.5	17.5	11.5
$\lambda/2$	2^9	2^{12}	6	3.5	7.2	4.5	21.2	15.2
$\lambda/4$	2^9	2^{13}	6	3.4	14.4	4.5	28.3	22.3

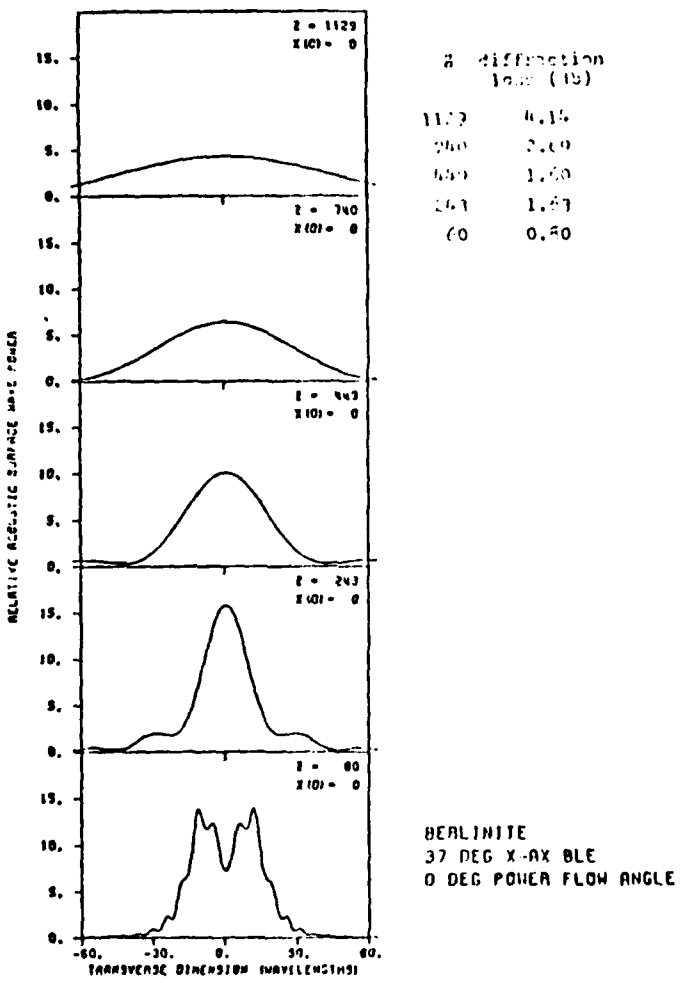

FIG. 22 Diffraction profiles for 37°, X-axis boule cut in berlinite. Z is in wavelengths. Transducer is 46 wavelengths wide and operates at 280 MHz. The appropriate diffraction loss for various Z values is indicated in dbs.

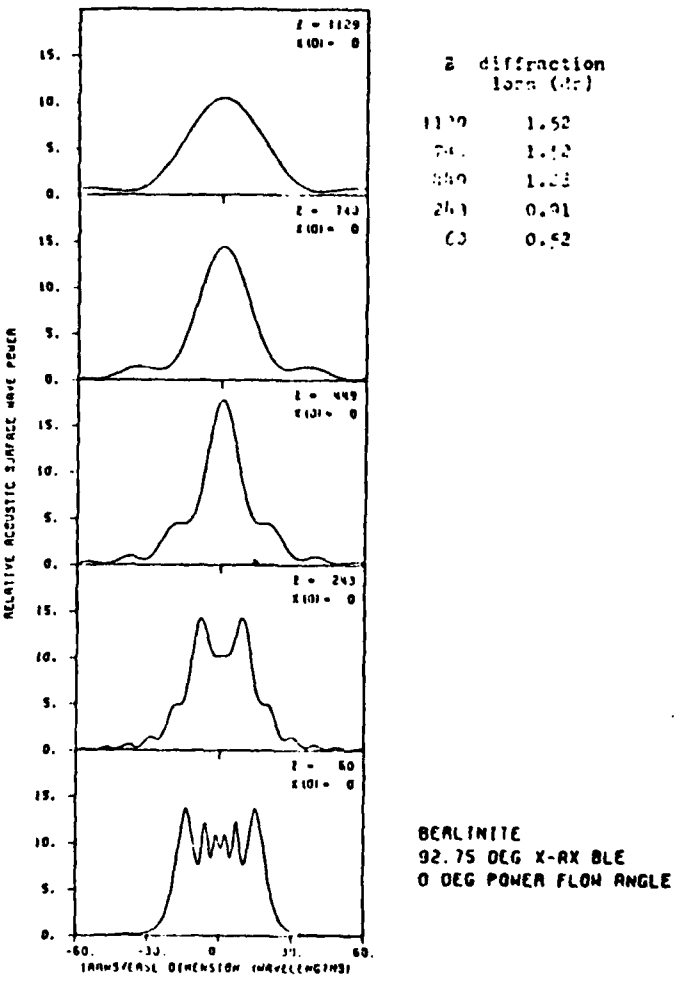

FIG. 23 Diffraction profiles for 92.75°, X-axis boule cut in berlinite. Definitions are the same as in Fig. 22

University of Maine, Orono not by AFOSR funds.

A laser probe system similar to that described by Szabo and Slobodnik[30] was developed. The major difference is that the lock-in amplifier is replaced by an inexpensive phase locked loop. A very complete description of the system may be found in reference 50.

The systems's operation has been verified thus far only with transducers fabricated on Y-Z lithium niobate. Results similar to those reported by Szabo and Slobodnik[30] were obtained. We hope to be able to check quartz shortly and ultimately berlinite.

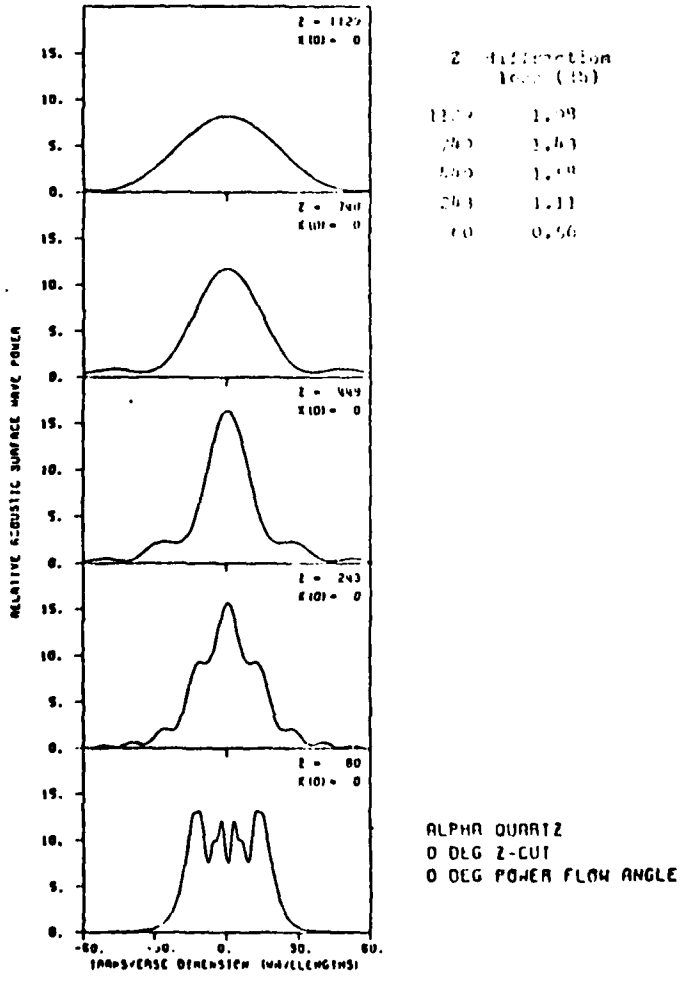

FIG. 24 Diffraction profiles for 0° Z-cut in α-quartz. Definitions are the same as in Fig. 22

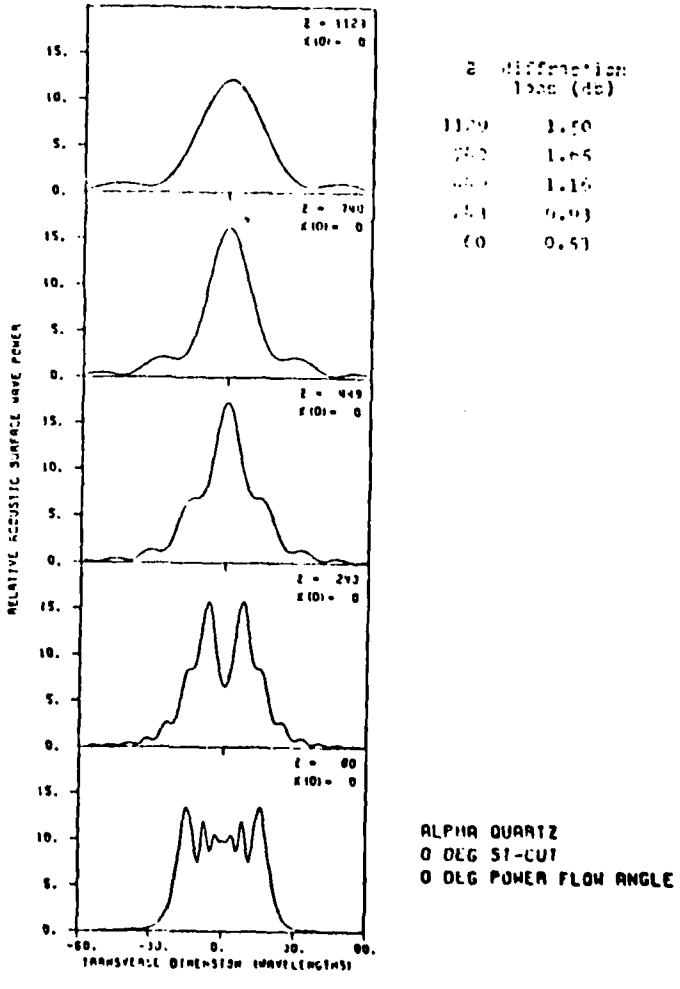

FIG. 25 Diffraction profiles for 0° ST-cut in α-quartz. Definitions are the same as in Fig. 22

E. Experimental Work on Berlinite

The theoretical calculations by the University of Maine group and others have shown berlinite to have piezoelectric coupling significantly higher than quartz and many temperature compensated cuts. This provided the motivation for the experimental study on berlinite.

One of the investigators (J.F. Vetelino) spent some time in Germany in 1976 and obtained samples of berlinite. These samples were grown by Prof. G. Lehmann at the University of Münster. These samples were brought to Mann Laboratory in Cambridge, Massachusetts for evaluation and for orientation of the crystals. A lengthy discussion with Edward Warekois and co-workers at Mann Labs concerning our needs with respect to the use of the crystals and their advice on the feasibility of implementing our needs proved to be very fruitful. Several pieces appeared to have some possibilities. In this section experimental SAW property results for the x-axis boule 85^{o}, 87.25^{o} and 90^{o} orientations are presented and discussed.

Experimental Measurements on the 75 MHz One Transducer Berlinite Sample

The one transducer technique[48] was used to measure k^2 on a berlinite plate oriented to x-axis boule, 87.25^{o}. Using an impedance bridge, a static capacity of 5.27 pf was found. The resulting conductance versus frequency curve is presented in Figure 26.

From Figure 26 it can be seen that the synchronous conductance was 0.27×10^{-3} mho's and occured at a frequency of 73.6 MHz. This implies that k^2 is 0.003. This can be shown to correspond to a $\Delta v/v$ of 0.13%. This is to be compared to a theoretical value[51] of .254%.

Experimental Measurements on the 90 MHz x-axis Boule 87.25^{o} Berlinite Sample

A 90 MHz delay line was fabricated on a berlinite plate oriented to x-axis boule, 87.25^{o}. The velocity was determined using the impulse technique. The

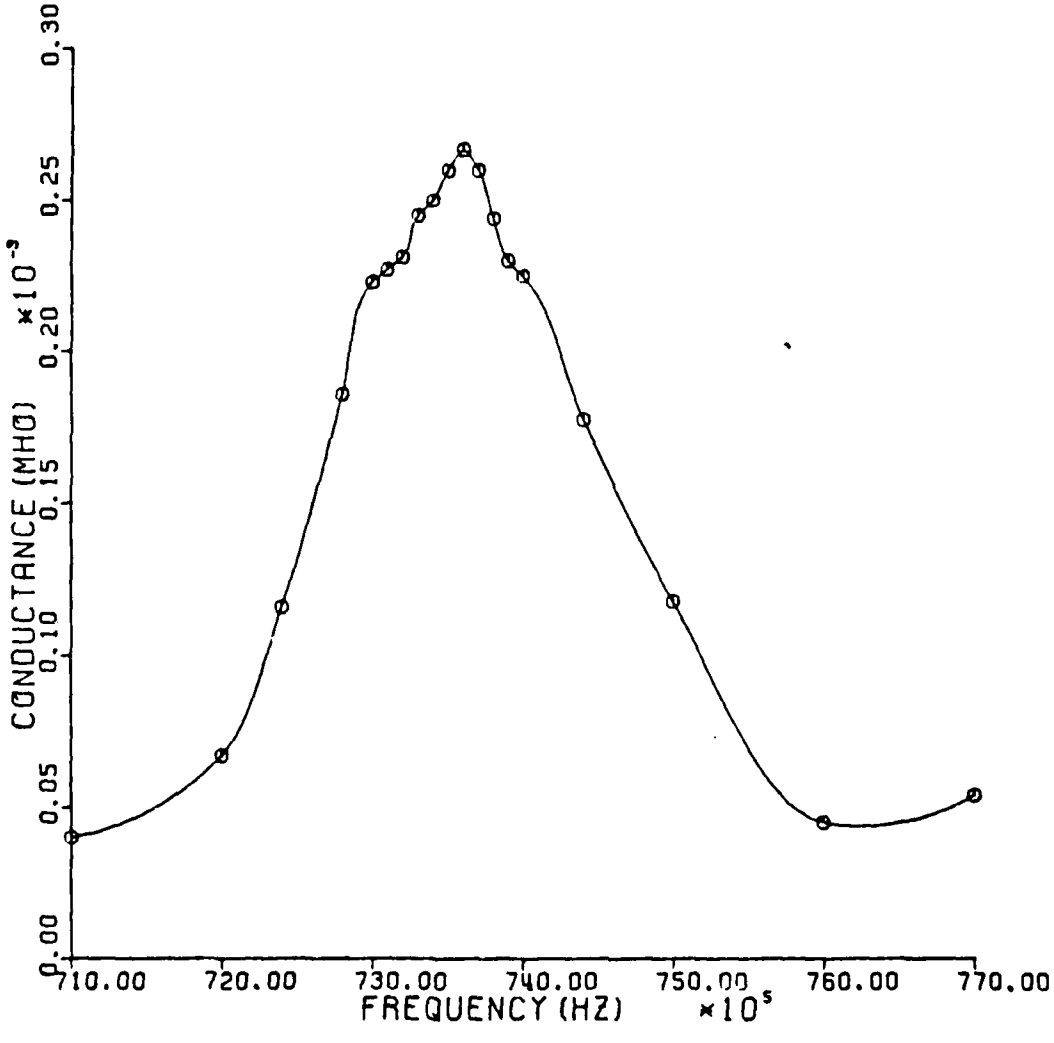

Fig. 26 Conductance versus frequency for 75 MHz berlinite IDT

distance between transducers, found using a traveling microscope, was 1.8244 mm. The time delay was found to be .664 microseconds. This corresponds to a SAW velocity of 2747 m/sec. as compared to a theoretical velocity[51] of 2741 m/sec.

The measurement of $\Delta v/v$ using the phase technique was not performed on this sample since its surface area was not large enough to accomodate the 60 MHz pattern.

The oscillator technique was used to determine the fractional time delay ($\Delta\tau/\tau$) as a function of temperature. The frequency versus temperature curve obtained is shown in Figure 27 and the corresponding $\Delta\tau/\tau$ curve is shown in Figure 28. Since the slope of the $\Delta\tau/\tau$ curve is TCD, temperature compensation can be seen to occur at approximately $32^{o}C$. This is to be compared to a theoretical temperature compensation of $25^{o}C$.

Experimental Measurements on the 90 MHz X-axis Boule 90^{o} Berlinite Sample

The impulse technique was also used on the 90^{o} orientation of berlinite. The distance between transducers was 1.8244 mm and the time delay was .66 microseconds. This corresponds to a SAW velocity of 2764 m/sec. as compared to theoretical value[51] of 2737 m/sec.

The oscillator technique was also used to determine $\Delta\tau/\tau$ versus temperature on the 90^{o} cut of berlinite. The resulting frequency versus temperature curve is shown in Figure 29 and the corresponding fractional time delay curve is shown in Figure 30. From the $\Delta\tau/\tau$ curve it can be seen that temperature compensation occurs at $40^{o}C$.

Experimental Measurement on the 60 MHz X-axis Boule 85^{o} Berlinite Sample

A 60 MHz delay line was fabricated on a berlinite plate oriented to x-axis boule, 85^{o}. Since this plate was the largest of the samples investigated, a larger delay line fits on the available surface area.

Using the impulse technique, the delay time was found to be .980 microseconds. Since the distance between transducers was 2.780 mm, the velocity

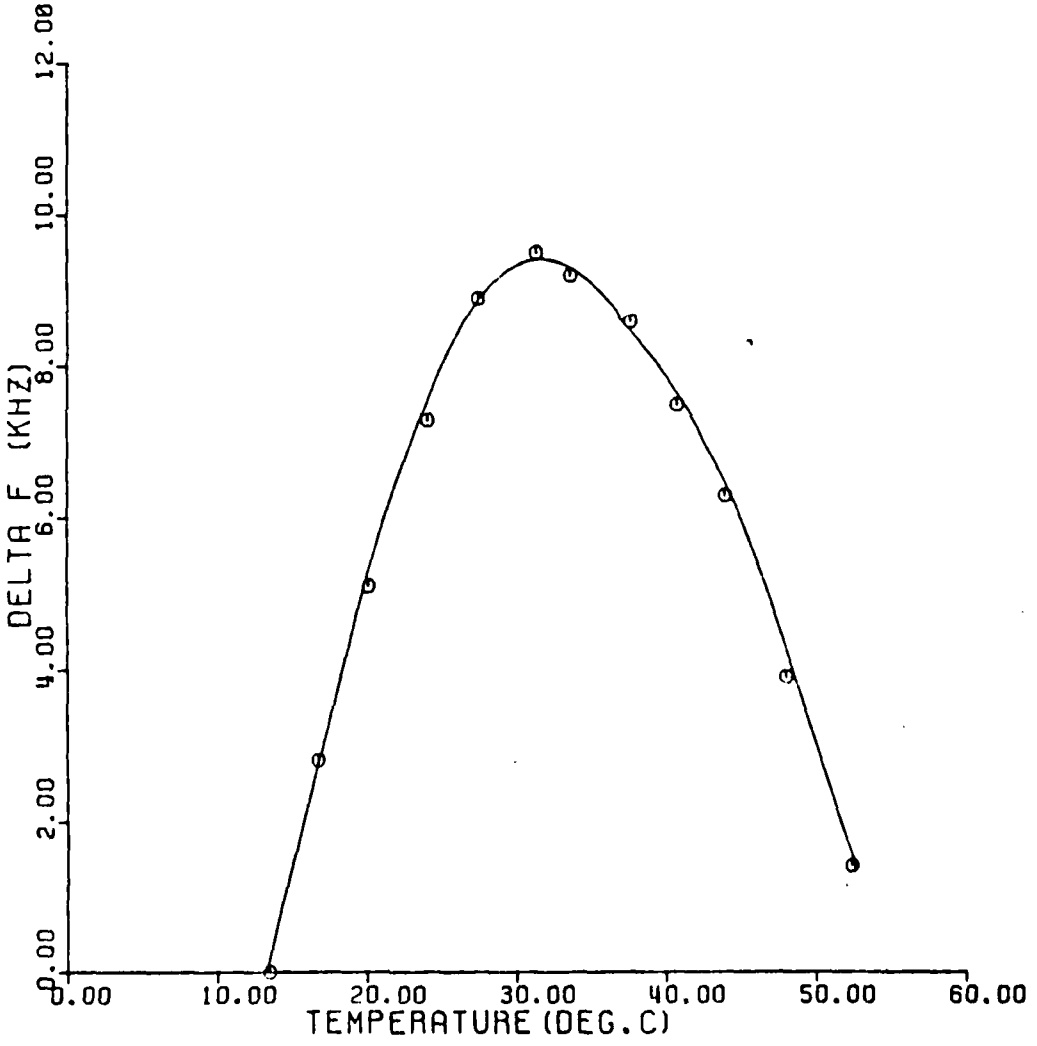

Fig. 27 Frequency versus temperature for berlinite 90 Mllz x-axis boule 87.25° delay line

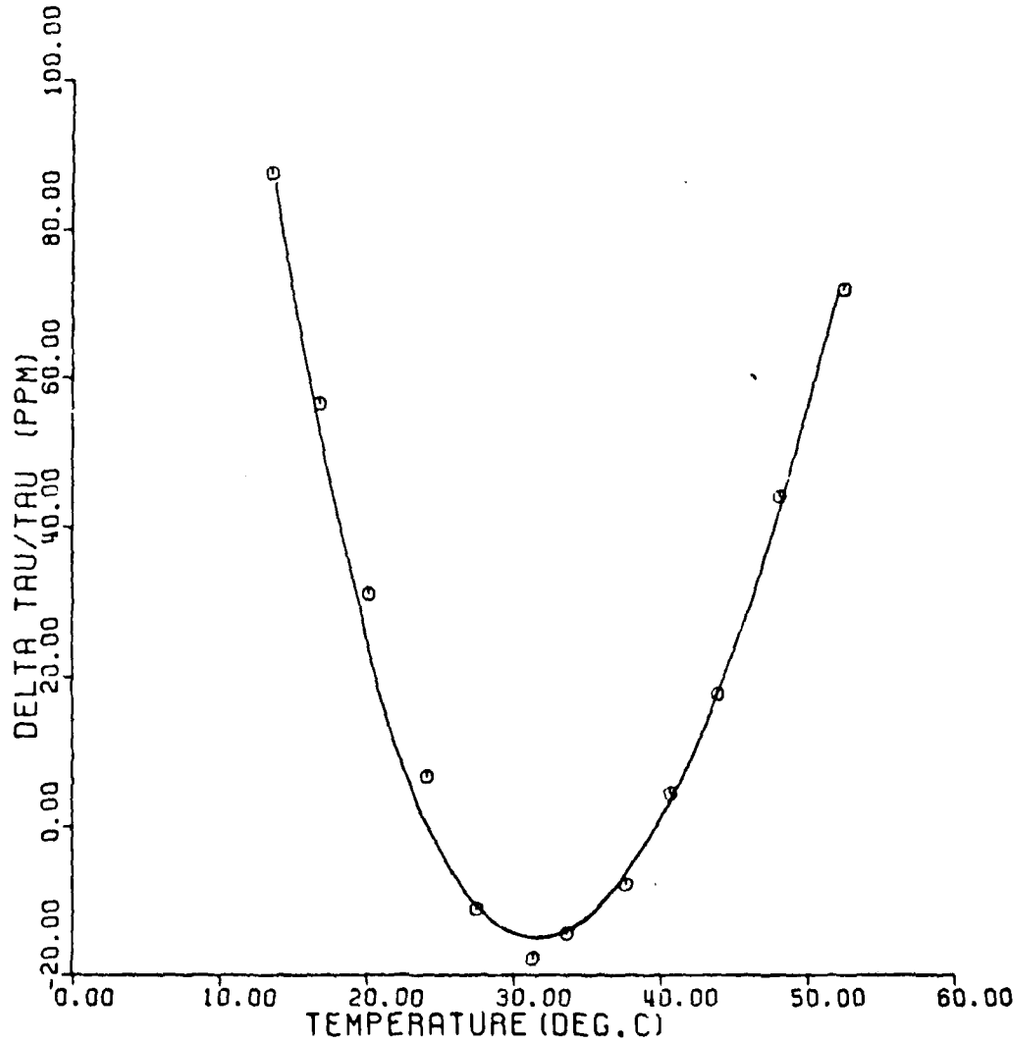

Fig. 28 Fractional time delay versus temperature curve for berlinite 90 MHz x-axis boule 87.25° delay line

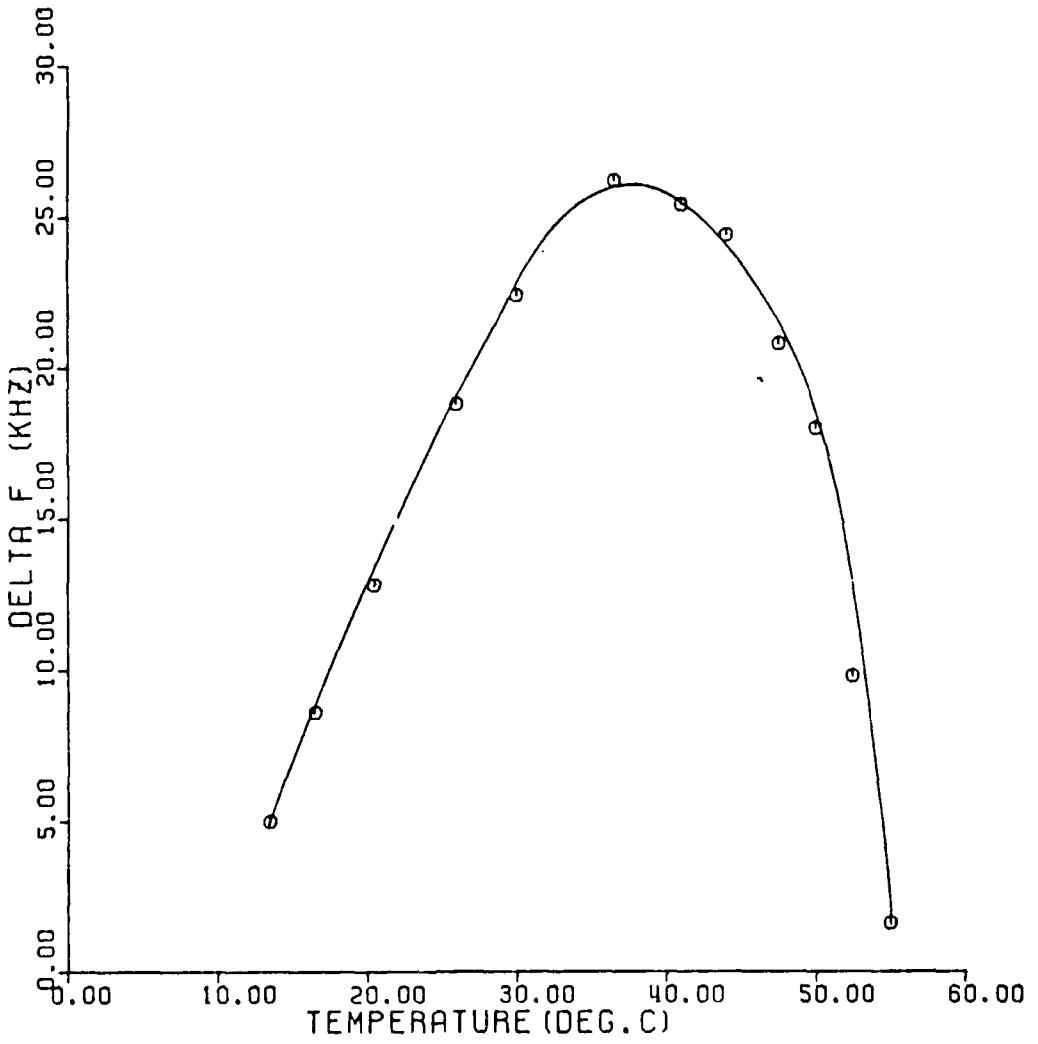

Fig. 29 Frequency versus temperature for berlinite 90 MIlz x-axis boule 90° delay line

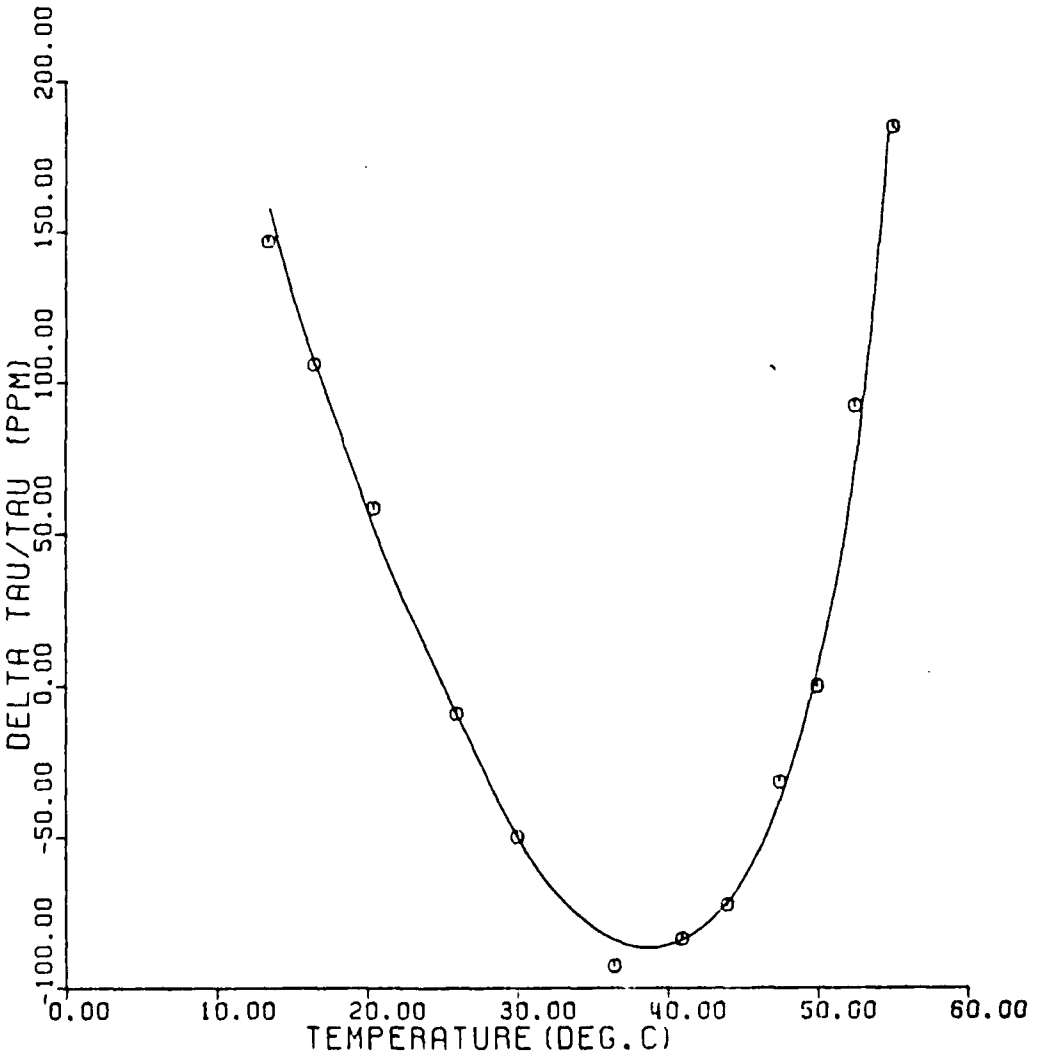

Fig. 30 Fractional time delay versus temperature for berlinite 90 MHz x-axis boule 90° delay line

was found to be 2836 m/sec. This is to be compared to a theoretical velocity[51] of 2744 m/sec.

Because of the increased distance between transducers, the phase technique[48] was used to measure the $\Delta v/v$ of the berlinite device. The width of the aluminum strip deposited was 0.6 mm and the resulting phase versus metal thickness curve is shown in Figure 31. Using these results, $\Delta v/v$ was found to be .11%. This is to be compared to a theoretical $\Delta v/v$[51] of .26%.

The oscillator technique was again used to determine the fractional time delay curve. Figure 32 shows the frequency versus temperature curve obtained and Figure 33 shows the corresponding $\Delta\tau/\tau$ curve. The resulting temperature compensation was found to occur at approximately 38°C.

Comparison of Experimental to Theoretical Results on Berlinite

The experimental results for the various orientations in berlinite are summarized in Table 5 and compared to the theoretical calculations by Jhunjhunwala *et al.*[51]

Discussion

From Table 5 it can be seen that our experimental results for berlinite are in reasonable agreement for the SAW velocity, poor agreement for $\Delta v/v$, and fair agreement for TCD. The velocity measurements on the 90 and 87.25 degree cuts of berlinite agree very well with the theoretically predicted velocities. In the case of the measurements on the 85 degree cut, our results do not agree as well. A reason for this might be that the 85 degree substrate was of poor quality.

It is interesting to note that in the case of $\Delta v/v$ measurements, two different techniques resulted in approximately the same value for $\Delta v/v$.

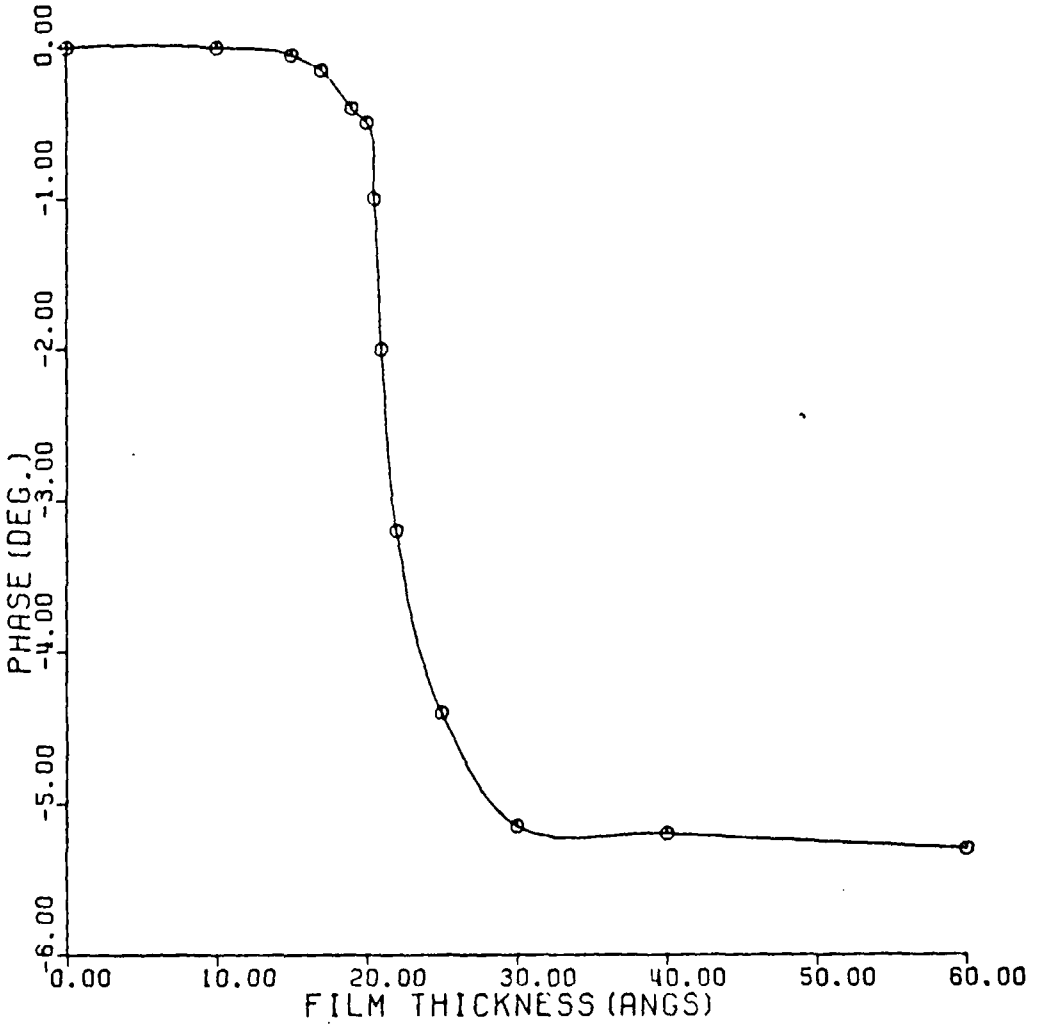

Fig. 31 Phase versus film thickness for berlinite 60 MHz x-axis boule 85° delay line.

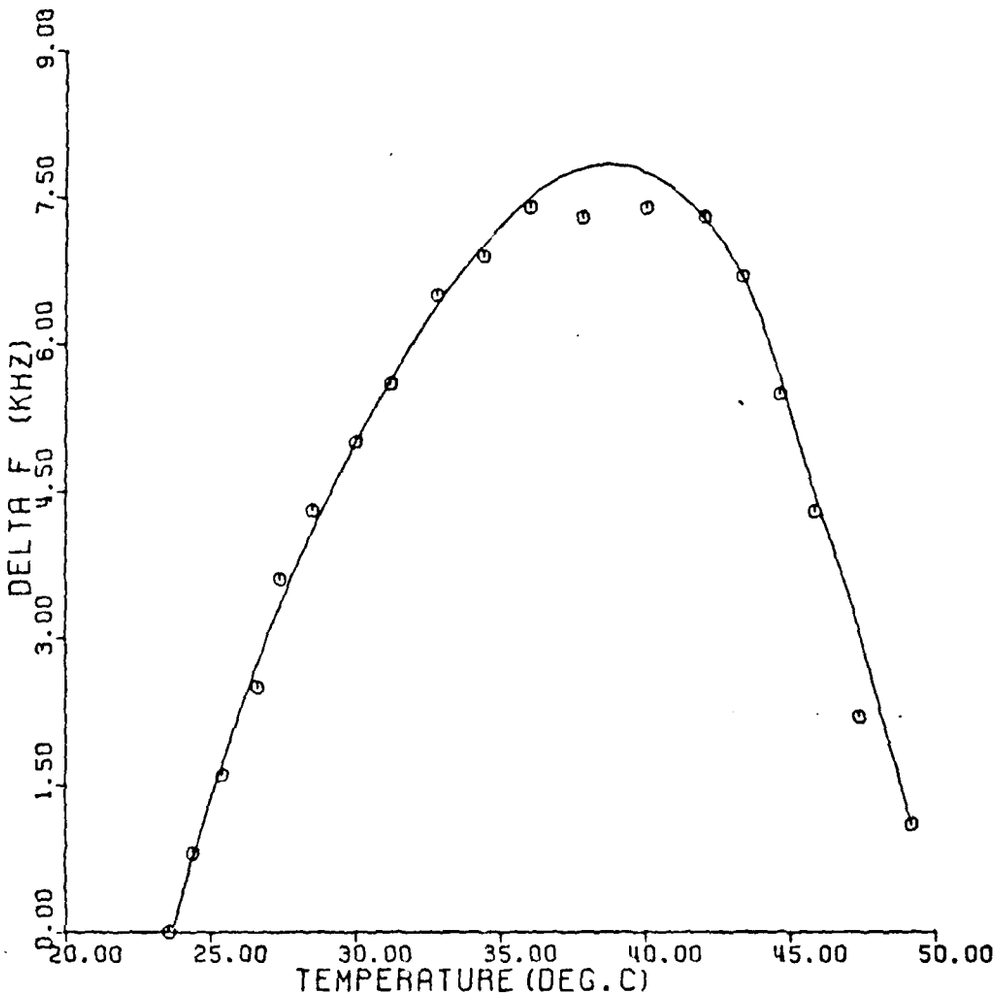

Fig. 32 Frequency versus temperature for berlinite 60 Mllz x-axis boule 85° delay line.

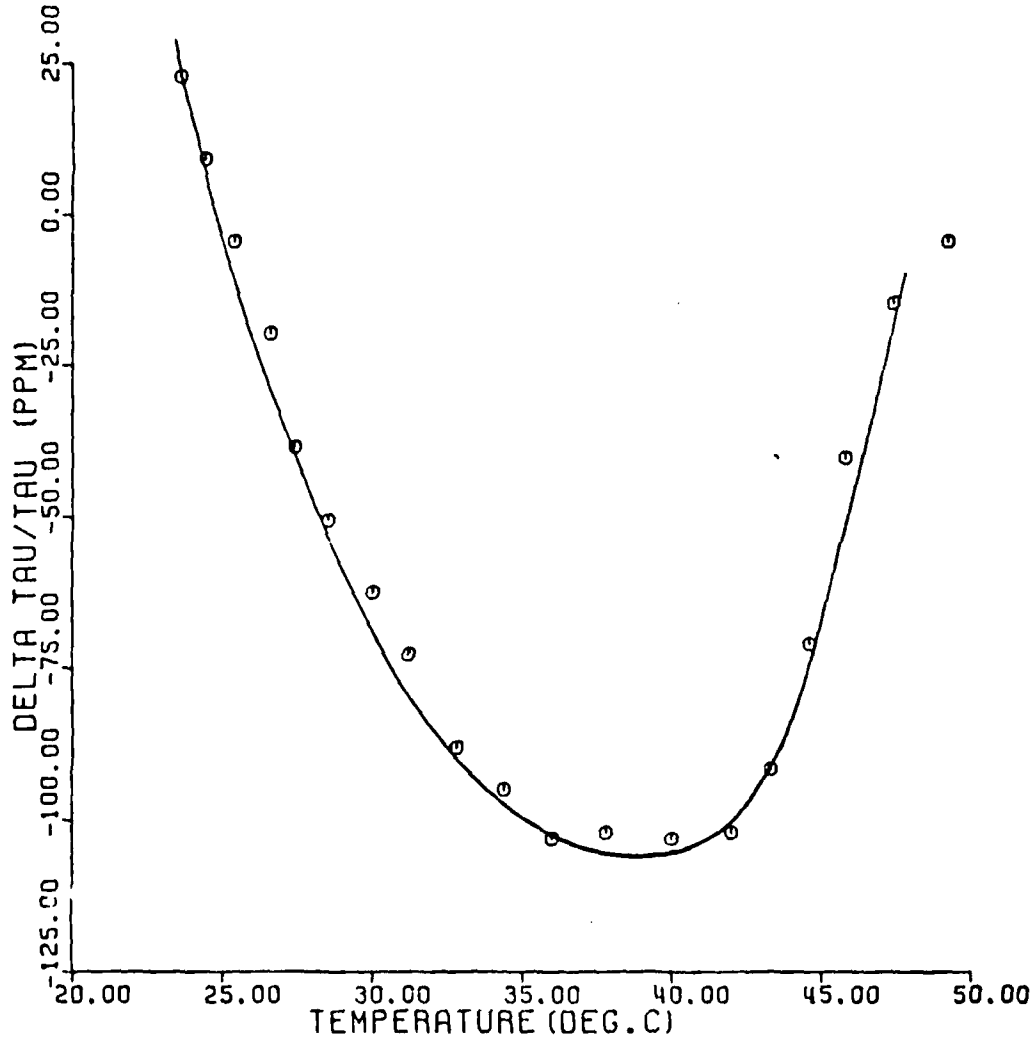

Fig. 33 Fractional time delay versus temperature for berlinite 60 MHz x-axis boule 85° delay line.

TABLE 5.

COMPARISON OF EXPERIMENTAL AND THEORETICAL RESULTS FOR THE THREE ORIENTATIONS OF BERLINITE STUDIED

Orientation	85° Exp.	85° Theo.[a]	87.25° Exp.	87.25° Theo.[a]	90° Exp.	90° Theo.[a]
Velocity (m/sec)	2836	2744	2747	2741	2764	2738
$\Delta v/v$ (%)	.11	.26	.13	.25	--	.247
TCD (ppm/°C)	11.3	-.18	3.3	-.11	10.	-.4
Temperature at which compensation occurs, (°C)	38.	--	32.	25.	40.	--

[a]Reference 51

The fact that these do not agree well with theory seems to indicate that the error is due to inaccurate input parameters and/or poor quality crystals.

Error also resulted between experimental and theoretical results for TCD. This could be due to either inaccurate temperature derivatives of the input data used to calculate the theoretical TCD or poor quality berlinite samples. In previous theoretical calculations for TCD performed by Carr et al.[52] and Jhunjhunwala et al.[51] the calculated results are slightly different. A small difference in input data can cause a difference in the calculated results for TCD. Therefore, it is important that the input data be extremely accurate.

In view of the present work, it is interesting to compare berlinite to other temperature compensated materials. To date the only temperature compensated materials are α-quartz, TeO_2, α-berlinite and the sulfo-salt materials. The best known of these is quartz and to a lesser extent, the sulfo-salt materials. TeO_2 has coupling five times less than quartz and hence is not useful in device applications.

Table 6 compares the SAW velocity and $\Delta v/v$ for temperature compensated cuts in quartz, Tl_3VS_4 and berlinite. In the case of Tl_3VS_4, the $\Delta v/v$ is very high but since the material is very soft, device fabrication is more difficult. In quartz the piezoelectric coupling is significantly less than that of berlinite. Berlinite has reasonable piezoelectric coupling, temperature compensation and no unusual fabrication problems.

Temperature stability over a temperature range is another parameter which must be considered in determining the usefulness of a material in SAW applications. This parameter is found by fitting parabolas to the $\Delta\tau/\tau$ curve of the material investigated, and using the second order coefficient as a

TABLE 6.

COMPARISON OF THE SAW PROPERTIES OF BERLINITE TO THOSE OF Tl_3VS_4 AND QUARTZ

Material	Crystallographic Orientation	SAW Velocity (m/sec)	$\Delta v/v$ (%)
Quartz[a]	ST-cut	3158 m/sec	.00058
Tl_3VS_4[b]	53°(110) cylinder cut	1033 m/sec	.4
Berlinite[c]	x-axis boule 87.25°	2733 m/sec	.25

[a]Results for SAW velocity and $\Delta v/v$ were obtained from Ref. 53

[b]Results for SAW velocity and $\Delta v/v$ were obtained from Ref. 54

[c]Results for SAW velocity and $\Delta v/v$ were obtained from Ref. 51

shaping factor. For ST-cut quartz the shaping factor was found to be .05. This is to be compared to the berlinite shaping factor which was .25. Although this seems to indicate that the TCD for quartz is low for a wider range of temperature than that for berlinite, it is possible that other cuts of berlinite have lower shaping factors. This phenomena is observed in the case of quartz.

Conclusions

Experimental surface acoustic wave measurements of velocity, TCD and $\Delta v/v$ have been performed on berlinite for the first time. These measurements have shown that berlinite does have temperature compensated cuts with piezoelectric coupling higher than that of quartz.

Experimental measurement of the SAW velocity was accomplished for three cuts of berlinite. The experimental value for $\Delta v/v$ was found to be only one-half of the theoretical value. This experimental value was still twice that of ST-cut quartz. One possible source of error for the discrepancy between theory and experiment might be inaccuracies of the input parameters used to calculate the theoretical value of $\Delta v/v$ or poor quality berlinite crystals.

Berlinite was shown to be temperature compensated. There was only fair agreement between the experimental and theoretical values for the temperature at which compensation occurs. Again the discrepancy might be attributed to inaccurate input data in theoretical calculations or poor quality berlinite crystals. It was also found that the steepness factor for berlinite was higher than that of quartz. This factor could however change dramatically for different cuts.

The present work has definitely shown that berlinite is a possible alternative material for quartz in applications requiring temperature compensation as well as reasonable piezoelectric coupling.

Large high quality berlinite crystals are however needed in order to make a more in-depth study of berlinite. In particular, an accurate determination of the temperature dependence of elastic, piezoelectric and dielectric constants of berlinite is needed so as to be able to better identify theoretical orientations which might be potentially useful for device applications. The larger crystals will also enable one to make a more in-depth experimental study of SAW parameters such as SAW velocity, $\Delta v/v$, TCD and insertion loss. Other material characteristics which should be performed include laser studies in order to obtain power flow, diffraction and attenuation profiles for various orientations. In order to improve the accuracy of the temperature measurements made, a more accurate set up is needed to control and monitor the temperature in the environmental chamber. A microcomputer could be used to control the temperature of the chamber as well as plot the resulting $\Delta\tau/\tau$ versus temperature curve. Finally, the availability of large crystals will enable berlinite SAW devices such as oscillators, resonators and filters to be fabricated and studied.

F. Surface Skimming Bulk Waves

The research work on SSBW began during the early summer of 1978 and is presently continuing under the sponsorship of the National Science Foundation. Some theoretical and experimental work was performed in part under the AFOSR sponsorship.

Theoretical Work

A theoretical analysis of the spectrum of waves excited by an IDT source on a piezoelectric half space was undertaken using an integral transform technique. The waves were of the surface and bulk type. A numerical technique was initially used to calculate the fields. However, the complexity

of the computation precluded the use of this technique for a large number of orientations. Another technique which makes use of the theory of complex variables was then applied to calculate the fields. The poles in the integrand were shown to correspond to a SAW and/or pseudo SAW while the branch points corresponded to SSBWs. The SSBW which is the surface component of the bulk waves, decays as the 1/2 or 3/2 power of the distance from the source. A coupling coefficient is defined for the SSBW. This parameter along with the SAW and pseudo SAW coupling coefficients relate to the surface potential due to these waves when their respective attenuation is taken into account. The TCD for the SSBW is defined and the procedure for its calculation is developed.

Currently the theory is being refined and computer programs are being developed to obtain the various properties associated with the SSBW. Some of the special features of some of the calculations performed are summarized in Table 7.

Experiment

SSBW propagation was experimentally investigated for orientations in quartz, $LiTaO_3$ and berlinite.

The measurement techniques utilized to determine the fundamental SSBW parameters included the impulse and coherent pulse superposition techniques for the determination of velocity, the phase and oscillator methods for the measurement of TCD and the impulse technique for the determination of the SSBW attenuation. Also the relationship of the transducer's conductance to the electromechanical coupling of the SSBW was explored.

The orientations examined included a 90° rotated 85° Y-cut of berlinite (B-85), a rotated 36° Y-cut of $LiTaO_3$ (LT-126), and several 90° rotated Y-cuts of quartz. For those orientations supporting SSBWs, the presence of spurious signals in the device response were investigated. For those orientations

TABLE 7. SUMMARY OF SIGNIFICANT RESULTS

Material/ Orientation	Wave	Property	Comments
Fresnoite ($Ba_2Si_2TiO_8$)	SAW and pseudo SAW	moderate coupling and velocity minimum TCD≃40ppm/°C	possible convolver applications due to high dielectric constants and moderate coupling
BSO ($Bi_{12}SiO_{20}$)	SAW and pseudo SAW	low velocity moderate coupling	possible use in long delay lines
$LiNbO_3$/ Z cut, 0°	SAW	v≃3808m/sec k_s^2≃0.0042	Experimentally SAW and pseudo SAW
	pseudo SAW	v≃4517m/sec k_s^2≃0.022 moderately high attenuation	observed. Ratio of coupling obtained≃2.6. Ratio of velocity obtained≃1.16. Good
	SSBW	p=3/2 for all SSBW and moderate k^2_{skim}.	correspondence between experimental and
	plate modes	a dense coupling peak at v≃4517m/sec.	theoretical results.
Quartz/ AT 90°	SSBW	p=1/2, k^2_{skim}≃0.007. TCD≃0	no SAW/pseudo SAW; matches experimental results.
Quartz/ ST 90°	SSBW	p=1/2, k^2_{skim}≃0.0095; main lobe of bulk wave power found on the surface.	no SAW/pseudo SAW; matches experimental results.
Quartz/ 145° rotated Y cut 90° propagating	SAW	v≃4656m/sec k^2_{sub}≃0.00028	no pseudo SAW; SSBW dominates SAW for 600 wavelengths.
	SSBW	v≃4656m/sec k^2_{sub}≃0.0115, p=1/2	p=0.36 found experimentally for a combination of waves.

TABLE 7 . (Con't.)

Material/ Orientation	Wave	Property	Comments
$LiTaO_3$/ 36^o	SAW	v≃3367m/sec, k^2_{sub} low	SAW close to a SSBW with low coupling;
	pseudo SAW	v≃3461m/sec, k^2_{sub}≃0.0184 low attenuation	combination wave. Strongly coupled pseudo SAW;
	SSBW	v≃3367m/sec, k^2_{skim}≃0.0003 p=1/2 other SSBW have moderate k^2_{skim} and p=3/2	matches experimental results
$LiTaO_3$/ Y rot cut, 126^o	SAW	v≃3133m/sec k^2_{sub}≃0.0004	Expected theor. results: High coupled combination of a pseudo SAW and SSBW. Low coupled SAW.
	pseudo SAW	v≃4211.6m/sec k^2_{sub}≃0.0043 low attenuation	Low coupled longitudinal SSBW. Matches experimental results.
	SSBW	v≃4211.6m/sec, k^2_{sub}≃0.25, p=1/2 v≃5552m/sec, k^2_{sub}≃26, p=3/2 other SSBW, moderate k^2_{sub}, p=3/2	
Fused Quartz layer/$LiNbO_3$ Y rot cut, 41.5^o		TCD≃0 at t_1≃10 and t_1≃15 wavelengths $(\Delta v/v)_{(a)}$≃0.037 in either case	highest known coupling for SAW on $LiNbO_3$ or layered structure

possessing a dominant SSBW response, the fundamental SSBW wave parameters were determined. The results of these measurements were subsequently compared to the values predicted by the various theoretical approaches as well as the values measured by the other investigators.

Surface skimming bulk waves were observed on all of the orientations examined in this investigation except for the 90^{o} rotated 85^{o} Y-cut of berlinite. For this orientation, no response was observed. This result is in agreement with the value of SSBW coupling predicted for this orientation by the exact spectrum of waves analysis.

Devices constructed on the remaining cuts exhibited spurious responses resulting from the reflection of acoustic energy from the reverse surface and the ends of the substrate. Angling of these surfaces and the application of acoustic absorbers were found to result in limited suppression of the spurious signals depending on the transducer configuration and the substrate geometry.

The rotated 36^{o} Y-cut of $LiTaO_3$ was observed to support several acoustic waves. Comparison of the experimental results to the predictions of the exact spectrum of waves analysis indicated the existence of both a transverse and a longitudinal SSBW as well as a SAW and a PSAW. The dominant response was found to be the result of a combination of the PSAW and the transverse SSBW. Since these two responses were essentially inseparable, the utilization of this orientation in device applications was considered questionable.

The principle waves excited on the 90^{o} rotated Y-cuts of quartz were found to be horizontally polarized SSBWs. In tables 8 and 9 the measured values for velocity and TCD for various cuts in this orientation are compared to other experimental measurements and theory. In figure 34 the experimental SSBW amplitude as a function of distance from the transducer is compared to theoretical results.

TABLE 8. A COMPARISON OF CALCULATED AND MEASURED SSBW VELOCITIES FOR SELECTED 90° ROTATED Y-CUTS OF QUARTZ.

Cut Identification	Calculated Velocity[a] (m/s)	Measured Velocity (m/s)		
		Present Work	Yen[b]	Lewis[c]
Q-30	3311	3305±5	3314	--
Q-39.5	3330	3338±8	--	3328
AT-90	5097	5099±11	5100	5108
ST-90	4993	4952±9	4990	--
Q-145	4656	4650±6	--	--

[a] Reference 55

[b] Reference 56

[c] Read from curves presented in reference 52.

TABLE 9. A COMPARISON OF CALCULATED AND MEASURED VALUES OF SSBW TCD FOR SELECTED 90° ROTATED Y-CUTS OF QUARTZ.

Cut Identification	Calculated Values[a] (ppm/°C)	Measured TCD (ppm/°C)		
		Present Work	Yen[b]	Lewis[c]
Q-30	-20.0	-28.7	--	--
Q-39.5	0.09	1.85	--	-0.05
AT-90	1.58	6.20	--	3.0
ST-90	-34.7	-31.1	-28	--
Q-145	-77.0	-76.0	--	--

[a] Reference 55

[b] Reference 56

[c] Read from curves presented in reference 57.

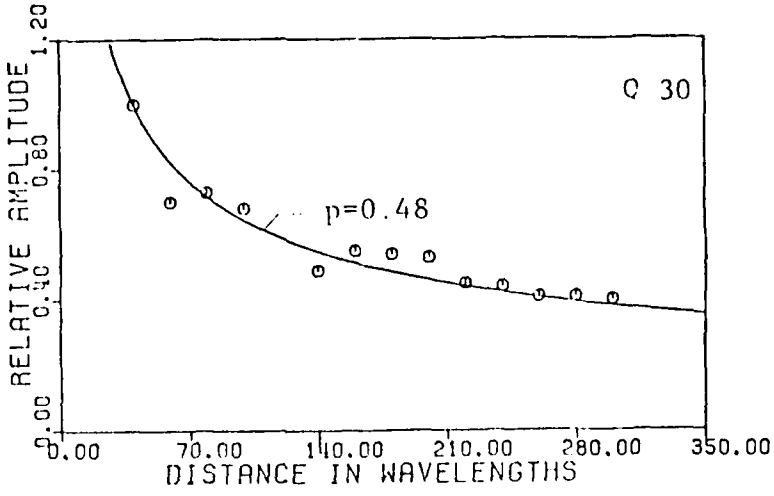

(a)

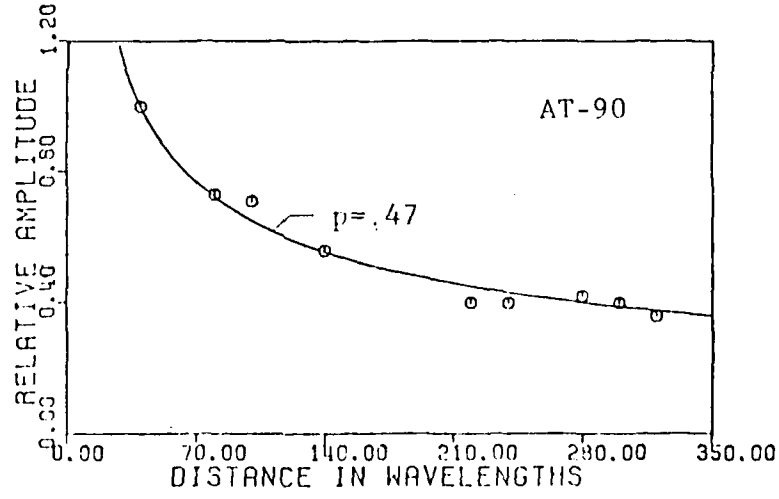

(b)

Figure 34 The variation of amplitude as a function of distance for the (a) Q-30 and (b) AT-90 cuts of quartz.

This investigation has demonstrated that the SSBWs supported by the 90^{o} rotated Y-cuts of quartz possess desirable properties. However, it has also been observed that the spurious signals which accompany the SSBWs represent a significant disadvantage. The suppression of these spurious signals by additional processing of the substrate reduces the desirability of the resulting device. Consequently, a considerable advantage must be demonstrated before SSBW devices can compete with the available technology for a particular application.

G. References

1. Nanamatsu, S., Doi, K. and Takahashi, M., Jpn. Jl. Appl. Phys. 11, 816 (1972)

2. Gupta, S.N., Vetelino, J.F., Field, J.C. and Jipson, V.B., 1974 Ultrasonics Symposium Proceedings, Milwaukee, p 291 (unpublished)

3. Slobodnik, A.J., USAF Cambridge Res-Labs. Report No. AFCRL-72-0092, 1971 (unpublished)

4. Haussühl, V.S., Phys. Status, Solidi 29, 159 (1968)

5. Jipson, V.B., Vetelino, J.F., Jhunjhunwala, A. and Field, J.C., Proc. IEEE 64, 568 (1976)

6. Soluch, W., Duracz, A., Lec', R., Field, J.C., Jhunjhunwala, A. and Vetelino, J.F., Proc. IEEE 65, 1093 (1977)

7. Mason, W.P., Piezoelectric Crystals and their Applications to Ultrasonics, D. Van Nostrand Co., Inc., New York, (1950)

8. Haussühl, V.S., Acta Cryst. A24, 697 (1968)

9. Volkova, E.N., Dianova, V.A., Zueu, A.L. and Izrailenko, A.N., Soviet Phys.-Crystallography 16, 284 (1971)

10. Jhunjhunwala, A., Vetelino, J.F. and Field, J.C., J. Appl. Phys. 48, 887 (1977)

11. See, for example, R.W.G. Wychoff, Crystal Structures, Vol. 3 (Interscience Publishers, 1965) p.31

12. Buerger, M.J., Amer. Min. 33, 751 (1948)

13. Flörke, D.W., Sci. Ceram. 3, 13 (1967)

14. Beck. W.R., J. Am. Ceram. Soc. 32, 147 (1949)

15. Buerger, M.J., Amer. Min. 39, 600 (1954)

16. Newnham, R.E., Ceram. Bull. 53, 821 (1974)

17. Chang, Z.P. and Barsch, G.R., IEEE Trans. Sonics Ultrasonics SU-23, 127 (1976)

18. Carr, P.H., Devito, P.A. and Szabo, T.L., IEEE Trans. Sonics Ultrasonics 19, 357 (1972)

19. Shiosaki, T., Kawabata, A. and Tanaka, T., Jap. Jl. Appl. Phys. 9, 631 (1970)

20. Araki, K. and Tanaka, T., Jap. Jl. Appl. Phys. 11, 472 (1972)

21. Vedam, J., Miller, D.L. and Roy, R., JAP 37, 3432-34 (1966)

22. Mort, J., JAP 38, 3414 (1967)

23. Yamada, T., JAP 46, 2894 (1975)

24. Barsch, G.R. and Spear, K.E., USAF Res. Lab. Report No. AFCRL-TR-75-0609 (1975)

25. Pratt, R.G., Simpson, G. and Crossby, W.A., Elect. Letters 10, 127 (1972)

26. Kraut, E.A., Tittman, B.R., Graham, L.J. and Lim, T.C., Appl. Phys. Letters 17, 271 (1970)

27. Slobodnik, A.J., Jr., Conway, E.D. and Delmonico, R.T., Microwave Acoustics Handbook, Vol. IA, USAF Res. Report No. AFCRL-TR-73-0597, Bedford (1973)

28. Slobodnik, A.J., Jr., Szabo, T.L., JAP 44, 2937 (1973)

29. Schweppe, H. and Quadfleig, P., IEEE Trans. Sonics Ultrasonics 21, 56 (1974)

30. Szabo, T.L. and Slobodnik, A.J. Jr., USAF Res. Lab. Report No. AFCRL-TR-73-0302 (1973)

31. Weinart, R.W. and Issacs, T.J., J. Elect. Mat. 5, 13 (1976)

32. Jhunjhunwala, A., Vetelino, J.F. and Field, J.C., Electronic Letters 12, 683 (1976)

33. Weinart, R.W., Private Communication (1976)

34. Issacs, T.J., Gottlieb, M., Daniel, M.R. and Feichtner, J.D., J. Elect. Mat. 4, 67 (1975)

35. Kimura, M., Fujino, Y. and Kawamura, T., Appl. Phys. Lett. 29, 227 (1976)

36. Eckstein, J., Recker, K. and Wallrafen, F., Naturwissensch 63, 438 (1976)

37. Kimura, M., J. Appl. Phys. 48, 2850 (1977)

38. Melngailis, J., Vetelino, J.F., Jhunjhunwala, A., Reed, T.B., Fahey, R.E. and Stern, E., Appl. Phys. Lett. 32, 203 (1978)

39. Stegeman, G. I., J. Appl. Phys. 47, 1712 (1976)

40. Jhunjhunwala, A., Vetelino, J.F. and Field, J.C., J. Appl. Phys. 48, 887 (1977)

41. Vetelino, J.F., Jhunjhunwala, A., and Field J.C., IEEE Ultrasonics Symposium Proc. Phoenix, 1977, pp 675-678

42. See, for example, Proc. IEEE, Special issue 64, No. 5 (1976)

43. See, for example, Budreau, A. J., 1974 Proc. IEEE Ultrasonics Symposium Proceedings, Milwaukee, p 299 (unpublished)

44. Sandbank, C.P. and Butler, M., Elect. Lett. 1, 501 (1971).

45. Parker, T.E. and Schulz, M.B., 1974 Proc. IEEE Ultrasonics Symposium Proceedings, Milwaukee, p 295 (unpublished); ibid. Appl. Phys. Lett. 26, 75 (1975)

46. Parker, T.E. and Wichansky, H., 1975 IEEE Ultrasonics Symposium Proceedings, Los Angeles, p 503 (unpublished)

47. Carr, P.H., Jhunjhunwala, A., Veilleux, L.A., Vetelino, J.F. and Field, J.C. 1977 IEEE Ultrasonics Symposium, Phoenix p 679-682 (1977)

48. Morency, D., Fabrication of and Microwave Measurement on Berlinite Surface Acoustic Wave Devices, MSEE Thesis, University of Maine, Orono, Maine (1978).

49. Raghavan, R.S., Temperature Compensation with Metal or Semiconductor Overlay on SAW Substrates, MSEE Thesis, University of Maine, Orono, Maine (1979).

50. Pelletier, J.A., Experimental and Theoretical Surface Acoustic Wave Diffraction Patterns, MSEE Thesis, University of Maine, Orono, Maine (1977)

51. Jhunjhunwala, A., Vetelino, J.F. and Field, J.C., 1976 IEEE Ultrasonics Symposium Proceedings, Annapolis, p 523; ibid J. Appl. Phys. Mar. 1977 (in press)

52. Carr, P.H. and O'Connell, R.M., 1976 Frequency Control Symposium Proceedings, Atlantic City, p 129

53. Slobodnik, A.J., USAF Cambridge Res. Labs. Report No. AFCRL-TR-73-0538, (1973).

54. Weinert, R.W., 1975 Frequency Control Symposium Proceedings, Atlantic City, p 139 (unpublished)

55. Jhunjhunwala, A. Doctoral Thesis University of Maine, Orono, Maine (1979).

56. Lau, K.F., Yen, K.H., Kasiwada, R.S. and Wang, W.L., 1977 IEEE Ultrasonics Symposium Proc., Phoeniz, Ariz. p 996 (1977).

57. Browning, T.I. and Lewis, M.F., 1977 Frequency Control Symposium Proc., p 258 (1977).

III. Personnel

Four faculty members and several graduate and undergraduate students have been involved in the research effort since February 15, 1975. Table 1 lists the various personnel along with their academic status and period of involvement.

Table 1. Personnel who have or are currently working on the research

Personnel	Academic Position	Involvement
John F. Vetelino	Associate Professor (Principal Investigator)	duration of the grant
John C. Field	Associate Professor (Principal Investigator)	Feb. 15, 1975 to June 1, 1978
Steven D. Mittleman	Assistant Professor	Aug. 1, 1977 to present
Waldemar Soluch	Visiting Professor	Jan. 1, 1978 to July, 1978
Ashok Jhunjhunwala	Graduate Student	Sept. 1, 1975 to Sept. 1, 1979
James Pelletier	Graduate Student	June 1, 1977 to Aug. 15, 1977
David Harmon	Undergraduate Student (Feb. 15, 1975 to Sept. 1, 1977)	duration of the grant
	Graduate Student (Sept. 1, 1977 to Sept. 1, 1979)	
Fabian Josse	Graduate Student	Sept. 1, 1977 to Sept., 1979
Donald Morency	Undergraduate Student (Feb. 15, 1975 to Sept. 1, 1976)	duration of the grant
	Graduate Student (Sept. 1, 1976 to Sept. 1, 1978)	
R. S. Raghavan	Graduate Student	Sept. 1, 1977 to Sept., 1979
Victor Jipson	Undergraduate	Feb. 15, 1975 to Sept. 1, 1975
Ronald Peabody	Undergraduate	June 1, 1977 to June 1, 1979
Louise Veilleux	Undergraduate	June 1, 1977 to June 1, 1979

The academic year involvement of the principal investigators was one quarter time or less while the summers were full time. The graduate student involvement averaged about one half time or less for the academic year and full time for the summers. The undergraduate students were part time during both the academic year and the summer.

IV. Degrees Granted

Ashok Jhunjhunwala	MSEE	June 1977
James Pelletier	MSEE	October 1977
Donald Morency	MSEE	October 1978
David Harmon	MSEE	December 1979
Ashok Jhunjhunwala	Ph.D.	December 1979
R. S. Raghavan	MSEE	December 1979
Fabian Josse	MSEE	December 1979

V. Scientific Papers Published

1. S.N. Gupta, J.F. Vetelino, V.B. Jipson and J.C. Field, "The Surface Acoustic Wave Properties of Lithium Gallium Oxide," in 1974 IEEE Ultrasonics Symp. Proc. (Milwaukee, WI), pp. 291-294.

2. S.N. Gupta, J.F. Vetelino, V.B. Jipson and J.C. Field, "Surface Acoustic Wave Properties of Lithium Gallium Oxide," J.Applied Physics, Vol. 47, pp 858-860, March, 1976.

3. V.B. Jipson, J.F. Vetelino, J.C. Field, D.G. Morency and D.L. Harmon, "The Surface Acoustic Wave Properties of $LiIO_3$," in 1975 IEEE Ultrasonics Symp. Proc. (Los Angeles, Calif.), pp 508-510.

4. V.B. Jipson, J.F. Vetelino, A. Jhunjhunwala and J.C. Field, "Lithium Iodate - A New Material for Surface Acoustic Wave Applications," Proc. IEEE, Vol. 64, pp 568-569, April 1976.

5. A. Jhunjhunwala, J.F. Vetelino and J.C. Field, "Berlinite, A Temperature Compensated Material for Surface Acoustic Wave Applications," in 1976 IEEE Ultrasonics Symp. Proc. (Annapolis, MD) pp 523-527.

6. A. Jhunjhunwala, J. F. Vetelino and J.C. Field, "Temperature Compensated Cuts with Zero Power Flow in Tl_3VS_4 and Tl_3TaSe_4," Electronics Letters, Vol. 12, pp 683-684, Dec. 1976.

7. A. Jhunjhunwala, J.F. Vetelino and J.C. Field, "Surface Acoustic Wave Properties of Berlinite," J. Applied Physics, Vol. 48, pp 887-892, March, 1977.

8. W. Soluch, A. Duracz, R. Lec, J.C. Field, A. Jhunjhunwala and J.F. Vetelino, "On the Temperature Coefficient of Delay for Surface Acoustic Waves in $LiIO_3$," Proc. IEEE Vol. 65, p 1093, July, 1977.

9. J.F. Vetelino, A. Jhunjhunwala and J.C. Field, "The Surface Acoustic Wave Properties of Bismuth Silicon Oxide," in 1977 IEEE Ultrasonics Symp. Proc. (Phoenix, Ariz.) pp 675-678.

10. P.H. Carr, A. Jhunjhunwala, L.A. Veilleux, J.F. Vetelino and J.C. Field, "New Low Loss High Coupling Mode up to 1 GHZ on $LiNbO_3$," in 1977 IEEE Ultrasonics Symp. Proc. (Phoeniz, Ariz.) pp 679-682.

11. J. Melngailis, J.F. Vetelino, A. Jhunjhunwala, T.B. Reed, R.E. Fahey and E. Stern, "Surface Acoustic Wave Properties of Fresnoite, $Ba_2Si_2TiO_8$," Applied Physics Letters 32, 203 (1978).

12. D. Morency, W. Soluch, J.F. Vetelino, S. Mittleman, D. Harmon, S. Surek and J.C. Field, "Experimental Measurement of the SAW Properties of Berlinite." Applied Physics Letters 33, 117 (1978).

13. D.G. Morency, W. Soluch, J.F. Vetelino, S.D. Mittleman, D. Harmon, S. Surek and J.C. Field, "Experimental Measurement of the SAW Properties of Berlinite" 1978 Frequency Control Symposium, Atlantic City, N.J., p 196-201.

14. D. Harmon, D. Morency, W. Soluch, J.F. Vetelino and S.D. Mittleman, "Experimental Determination of the SAW Properties of X-axis Boule Cuts in Berlinite", 1978 IEEE Ultrasonics Symposium, Philadelphia, Penn., (594-597) Sept. 25-27 (1978).

15. A. Jhunjhunwala, J.F. Vetelino, D. Harmon and W. Soluch, "Theoretical Examination of Surface Skimming Bulk Waves" 1978 IEEE Ultrasonics Symposium, Philadelphia, Penn. (670-674) Sept. 25-27 (1978).

16. D.L. Harmon, F. Josse and J.F. Vetelino, "Surface Skimming Bulk Waves in Y-rotated Quartz-Experimental Characterization and Device Implementation" 1979 IEEE Ultrasonics Symposium (in press).

VI. Scientific Interactions

In this section a short description of conferences attended, along with seminars and/or discussions with individuals or groups of scientists is presented. These items are presented in chronological order.

1. Surface Acoustic Wave Properties of Piezoelectric Materials

   Date - January 24, 1975

   Place - RADC/EEA, Deputy for Electronic Technology, Hanscom AFB, Mass.

   People - J.F. Vetelino, J.C. Field and V.B. Jipson - University of Maine
   Paul Carr, Andrew Slobodnik and other members of the SAW Group - RADC/EEA Deputy for Electronic Technology Hanscom AFB, Mass.

   Subject Matter - Discussions were held with Paul Carr's SAW Group at RADC. Problems relating to the different modes propagating on the surface of the piezoelectric substrate and the identification of new piezoelectric materials were some of the topics discussed.

2. Surface Wave Guiding Structures*

   Date - April 24, 1975

   Place - University of Maine

   People - Members of the University of Maine SAW Group
   Arthur A. Oliner - Polytechnic Institute of New York, Brooklyn, New York.

   Subject Matter - Arthur Oliner was invited to give a seminar on waveguiding structures. While he was at the University discussions were held on mutual problems of interest in the area of surface acoustic waves.

3. 1975 IEEE Ultrasonics Symposium

   Date - Sept. 22-24, 1975

   Place - Los Angeles, California

   People - John F. Vetelino and J.C. Field - University of Maine

   Subject Matter - A paper on the surface acoustic wave properties of $LiIO_3$

(see Section V. No. 3) was presented. Many fruitful discussions were held with colleagues working in the area of SAWs.

4. Theory and Fabrication of SAW Devices

Date - Sept. 25, 1975

Place - Hughes Aircraft Co., Fullerton, Calif.

People - John F. Vetelino and J. C. Field - University of Maine
Tom W. Bristol and W. Jones - Hughes Aircraft Company, Fullerton, Calif.

Subject Matter - Discussions were held on fabrication problems and techniques and the theory of pseudo SAW modes propagating on piezoelectric crystals.

5. New High Velocity SAW Devices

Date - Sept. 26, 1975

Place - University of Southern California, Los Angeles, Calif.

People - John F. Vetelino and J.C. Field - University of Maine
Ken Lakin and members of his SAW Group - University of Southern California, Los Angeles, California.

Subject Matter - New high velocity single crystals and layered SAW Devices and appropriate fabrication techniques.

6. $LiIO_3$ SAW Device Fabrication and SAW Convolvers

Date - November 12, 1975

Place - MIT Lincoln Laboratory, Lexington, Mass.

People - J.F. Vetelino and J.C. Field - University of Maine
Ernest Stern, John Caffarella and other members of the SAW Group - MIT Lincoln Laboratory, Lexington, Mass.

Subject Matter - Discussions were held relating to the problems in the fabrication of $LiIO_3$ SAW devices. The design of SAW convolvers

and the application of SAWs for measuring surface semiconducting properties such as mobility and conductivity were also discussed.

7. Metalization Problems in SAW Devices**

Date - April 19, 1976

Place - Institut fur Angewandte Festkorperphysik, Freiburg, West Germany

People - J.F. Vetelino - University of Maine

William H. Haydl and members of his SAW Group.

Institute fur Angewandte Festkorperphysik, D-78, Freiburg, West Germany.

Subject Matter - J.F. Vetelino was invited to give a talk on new materials for surface acoustic wave applications. Discussions were held with William and members of his group with regard to surface metalization and the effect it has on the performance of SAW devices such as SAW oscillators, resonators and narrowband filters.

8. Theory of Surface Acoustic Waves**

Date - May 26, 1976

Place - Tele and Radio Research Institute, Ratuszowa 11, Warsaw, Poland

People - J.F. Vetelino - University of Maine

Waldemar Soluch and members of his piezoelectric filter group - Tele and Radio Research Institute, Ratuszowa 11, Warsaw, Poland.

Subject Matter - J.F. Vetelino was invited to present a seminar on the theory of surface acoustic waves. Discussions were held on $LiIO_3$ and other new materials which are under investigation in Waldemar Soluch's group.

9. New Materials for Surface Acoustic Wave Applications**

Date - July 5, 1976

Place - Univerisity of Koln, Koln, West Germany

AD-A082 079 MAINE UNIV ORONO DEPT OF ELECTRICAL ENGINEERING F/G 9/3
MICROWAVE SURFACE ACOUSTIC WAVE MATERIALS.(U)
FEB 80 J F VETELINO AFOSR-75-2816
UNCLASSIFIED AFOSR-TR-80-0135 NL

2 2

END
DATE FILMED
4 80
DTIC

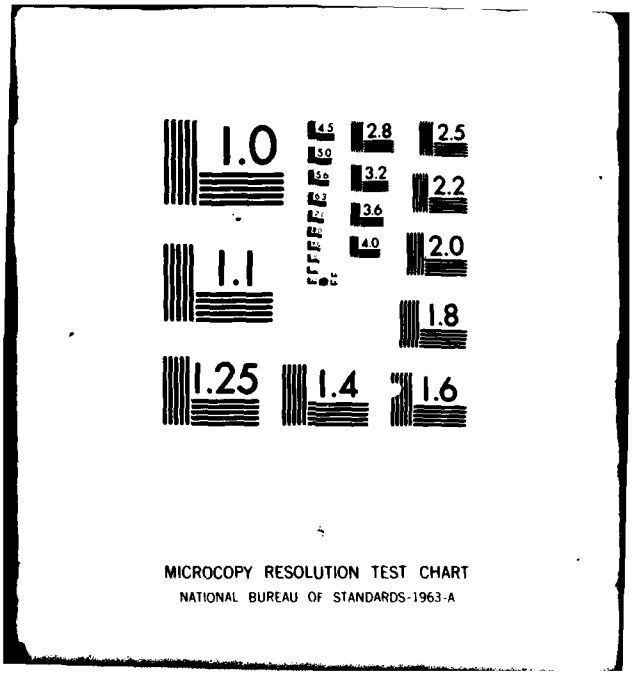

People - J.F. Vetelino - University of Maine

S. Von Haussühl - University of Koln, Koln, West Germany

Subject Matter - J.F. Vetelino was invited to give a seminar on new materials for SAW spplications. Prof. Von Haussühl, who is a crystallographer and a physicist, has grown many crystals. Discussions centered upon those materials which might be useful for SAW applications.

10. 1976 IEEE Ultrasonics Symposium

Date - Sept. 28 to Oct. 1, 1976

Place - Annapolis, Maryland

People - John F. Vetelino and J.C. Field - University of Maine

Subject Matter - A paper on the surface acoustic wave properties of berlinite (see section V No. A-5) was presented. Many fruitful discussions were held with colleagues working in the area of SAWs.

11. New Material for SAW Convolvers

Date - Nov. 19, 1976

Place - MIT Lincoln Laboratory, Lexington, Mass.

Subject Matter - The discussion centered about the possibility of obtaining a new material for SAW convolver applications. In particular, those materials which would enable one to have a larger time bandwidth product were discussed.

12. The Potential of Berlinite for SAW Applications

Date - Jan. 14, 1976

Place - RADC/EEA Deputy for Electronic Technology, Hanscom AFB, Mass.

People - J.F. Vetelino, Paul Carr and members of the crystal growing group at RADC.

Subject Matter - The discussion involved the possible use of berlinite in

SAW applications. The possibilities of obtaining single crystal samples of berlinite along with the problems and techniques of growing berlinite were discussed.

13. SAW Fabrication Facility - Equipment and Techniques

Date - July 25, 1977

Place - RADC/EEA Deputy for Electronic Technology, Hanscom AFB, Mass.

People - John F. Vetelino, Steven D. Mittleman, Don Morency and Dave Harmon - University of Maine

Jose Silva, William Kearns and Alan Budreau - RADC/EEA Deputy for Electronic Technology

Subject Matter - Discussions involved equipment and facilities appropriate for clean room and fabrication of SAW devices. The University of Maine is seriously thinking of obtaining a clean room for SAW fabrication.

14. SAW Fabrication Facility - Equipment and Techniques; Fresnoite, a New Material for SAW Convolver Applications

Date - July 26, 1977

Place - MIT Lincoln Laboratory, Lexington, Mass.

People - John F. Vetelino, Steven D. Mittleman, Don Morency and Dave Harmon - University of Maine

John Melngailis, John Caffarella, Ernest Stern, Manfred Schulz, Richard Williamson and members of the SAW fabrication group - MIT Lincoln Laboratory

Subject Matter - Discussions involved equipment and facilities appropriate for a clean room facility, the theoretical study of the SAW properties of fresnoite and advantages and disadvantages of using layered structures for SAW devices.

15. Crystal Preparation on Berlinite for SAW Applications

Date - August 2, 1977

Place - Mann Laboratories, Cambridge, Mass.

People - J.F. Vetelino, Steven D. Mittleman, Don Morency and Steven Surek - University of Maine

Edward Warekois - Mann Laboratories

Subject Matter - Crystals of berlinite were brought to Mann Laboratories to study their potential in a SAW device. These crystals were x-rayed and proper orientations were placed on the crystals.

16. 1977 IEEE Ultrasonics Symposium

Date - Oct. 26-28, 1977

Place - Phoeniz, Arizona

Subject Matter - Two papers were presented, one on the surface acoustic wave properties of bismuth silicon oxide (see section V No. 9) and the other on a new low loss high coupling mode up to 1 GHZ on $LiNbO_3$ (see section V No. 10). Many fruitful discussions were held with colleagues working in the area of SAWs.

17. 1978 Frequency Control Symposium

Date - May 31 - June 2, 1978

Place - Atlantic City, New Jersey

Subject Matter - A paper was presented on experimental measurements of the SAW properties of berlinite.

18. 1978 IEEE Ultrasonics Symposium

Date - Sept. 25 - 27, 1978

Place - Philadelphia, Pennsylvania

Subject Matter - Two papers were presented, one the experimental determination of the SAW properties of x-axis boule cuts in berlinite and

the other on theoretical examination of surface skimming bulk waves.

19. 1979 Specialist Conference on Case Studies in Advanced Signal Processing

Date - Sept. 17-21, 1979

Place - Peebles, Scotland

Subject Matter - Attended a specialist conference by invitation and had many fruitful discussions with scientist from the US and abroad.

20. 1979 IEEE Ultrasonics Symposium

Date - Sept. 26-28, 1979

Place - New Orleans, Louisiana

Subject Matter - Three papers presented - (i) Surface skimming bulk waves in y-rotated quartz-experimental characterization and device implementation; (ii) Spectrum of acoustic waves emanating from a line source on a piezoelectric substrate and (iii) temperature and frequency control with metal and semiconducting films on SAW substrates.

*Scientific interaction relating directly to the research but travel not supported by the Air Force.

**These scientific interactions occurred while J.F. Vetelino was in Europe during the interval Jan.-July 1976. Expenses occurred as a result of these interactions were not supported by the Air Force.

VII. Relevant Information

The support rendered by the Air Force has enhanced the SAW effort at the University of Maine and enabled members of the SAW group to solve state of the art problems and interact personally with many fellow workers in both the United States and Europe. As a direct result of the expertise gained while working under the Air Force contract, we have been requested by MIT Lincoln Laboratory (Ernest Stern's group) to perform a theoretical study of the SAW properties of Fresnoite. This material is felt to have excellent potential in convolver applications. The Naval Underwater Systems Center at Newport, Rhode Island has hired one of the principal investigators (J.F. Vetelino) to act as a consultant in the area of surface acoustic waves and their possible application to sonar technology. The National Science Foundation has recently awarded Dr. Vetelino a two-year research grant on SSBW research. Recently, members of the SAW group have collaborated with Dr. Paul Carr at RADC in a SAW problem of mutual interest which resulted in a joint publication.

Both undergraduate and graduate students alike have benefitted from the SAW research. One undergraduate student (Victor Jipson) received a National Science Foundation Fellowship to obtain his Ph.D. degree. The four publications he had in the area of SAWs while he was an undergraduate student no doubt was one of the key factors enabling him to obtain the NSF Fellowship. The SAW research program has also enabled several undergraduates to participate in SAW research under a National Science Foundation Undergraduate Research Participation grant. One undergraduate was supported during the summers of 1975 and 1976, and three students were supported during the summers of 1977, 1978 and 1979. Previous students who worked in the SAW group are now at institutions like MIT, Cornell University, Stanford University, Lincoln Laboratory and Bell Laboratories.

The SAW program at the University of Maine has also attracted well known scientists in the area of microwave acoustics. Dr. Waldemar Soluch of the Tele and Radio Research Institute in Warsaw, Poland spent the 1978 spring semester at the University of Maine. Dr. Ryszard Lec' of the Polish Academy of Science will spend one year with the group starting in Jan., 1980. Dr. Bakhtiyar Umarov of the Physical-Technical Institute of the Academy of Sciences of the Tadzhik, Dushanbe, USSR will spend three months with the group starting in Jan., 1980. The interactions with these scientists will, no doubt, enhance the research efforts of the group.